Two Dimensional Depletion Interactions with Attractive Depletants

By

Maxwell Andreas Pinz

A thesis submitted to Johns Hopkins University in conformity with the requirements for the degree of Masters of Science in Engineering

Baltimore, Maryland

August 12 2015

Abstract

The objective of this thesis is to be able to characterize two dimensional depletion forces at an interface and determine what, if any, effect attraction between depletants has on depletion interaction. We decided to investigate attractive depletants as we wanted to determine how colloids adsorbed to an interface would be depleted with nano-scale depletants undergoing Van der Walls attraction. To accomplish this goal we wrote simulations to test various conditions for depletion in a two dimensional system. In this system we were able to define parameters such as the area fraction of the depletants, size ratio between the colloids and the depletants, and interactions between depletants. We then developed a theory to predict the interactions between the colloids as a function of the system parameters and depletant-depletant interactions. This theory pieces together several other well-known depletion papers. We start with the A.O theory to ensure that our simulation is working properly. Then we build up to using an adsorption interaction theory used for polymer chain depletants developed by Lekkerkerker et al. Finally, to utilize this theory, we had to predict how the colloids would alter the depletant density profiles around them; which meant incorporating a theory from Glandt et.al to predict how depletants pack around an object. This allowed us to predict the density profiles of depletants around colloids. We can take these density profiles and use the adsorption theory to determine how depletant-depletant attraction effects the depletion interaction profile between colloids. We then were able to determine from the interaction potential the contact forces of the colloids as well as their second virial coefficients. This can help us determine if depletant-depletant attraction can be used to modify the depletion force to aid in single domain crystal formation.

Advisors: Michael Bevan, Joelle Frechette

Committee: Michael Bevan, Joelle Frechette

Acknowledgements:

I would like to thank my mother, father, and brother for supporting me throughout my time here at Johns Hopkins. They have always been there for me and have been the impetus to put forth my best effort.

I would like to thank Michael Bevan and Joelle Frechette for welcoming me into their labs this past year and helping me navigate my way through my master's program.

I would like to thank all of the members of my labs for helping guide me through academia this past year. Whenever I had a question they were always more than willing to stop what they were doing and help me: Brad Rupp, Yuguang Yang, Xiaoqing Hua, Anna Coughlan, Matthew Petroff, Samantha Brandon, and Isaac Torres-Diaz.

Finally I would like to thank all of my friends I have made at Johns Hopkins over the past 5 years. The people at this university are what make it truly great. I have encounterd the smartest, kindest and most talented people I have met in my life. I doubt I will be so lucky as to encounter a collection of such diversely talented people anywhere else.

List of symbols and variables

ΔA - Change in center excluded area of depletants

a_c - Radius of a colloid

a_d - Radius of a depletent

f_i - Frequency of state i

g_i - Degeneracy of state i

$g_{cc}(\mathrm{r})$ - Radial distribution function between colloids

$g_{cd}(\mathrm{r})$ - Radial distribution function between colloids and depletants

$g_{dd}(\mathrm{r})$ - Radial distribution function between depletants

F_{cc} - Force between colloids

n - Number of depletants in a simulation

N_i - Number of counts in a particular state i

P_{ij} - Transition probability from state i to state j (in an infinite number of steps)

u_{cc} - Interaction potential between two colloids

u_{cd} - Interaction potential between colloid and depletant

u_{dd} - Interaction potential between two depletants

ΔV - Change in center excluded volume (3D depletion)

x - Fraction between surfaces between colloids

θ_1 - Angle that marks the boundary of the center excluded area

η - Area fraction of macromolecules at the interface

β_2 - Second viral coefficient for density expansion near the surface of a colloid.

β_{cc} - Second virial coefficient of colloids

β_{HD} - Second virial coefficient for hard disks

ρ - Number density of particles at a given point in space

ρ_b - Bulk number density of particles

Π - Osmotic pressure of macromolecules

kT - Boltzmann's constant*temperature

Table of Contents

List of figures and tables

1 Introduction

Depletion forces are important to the field of colloidal science and better understanding them will lead to a better understanding of interactions in a colloidal suspension[1] . The effect of a polymer to increase flocculation in a solution has been known since 1925[2] and the reversibility of this flocculation was discovered in 1939[3]. The reversibility of this flocculation showed that the force responsible for flocculation was relatively weak as it did not need to be sonicated. Early attempts to quantify this phenomena were incomplete [4-5] until Asakura and Oosawa developed their depletion theory in 1954[6]. This theory was elegant in its simplicity, and was remarkably accurate in predicting the flocculation conditions of different particles. In 1958, Asakura and Oosawa improved upon their theory to take into account the increased osmotic pressure of charged depletants, as well as polymer chain depletants[7]. Recently, advances in predicting macromolecule density profiles around larger objects[8] has led to the discovery of a repulsive aspect of some depletion interactions [9]. However most of the research devoted to depletion interactions is for a 3D system. We believe that depletion interactions in a 2D system are important to the surface characteristics of irreversibly adsorbed particles at an interface. While only occupying a very small fraction of any system, interfaces are critical to the behavior of a system[10].

Understanding depletion forces at an interface could aid our understanding of the formation and stability of colloidal crystals at interfaces. One field of interfacial science that is garnering a lot of attention is how to create 2D single domain crystals. The goal of current research is to create self-assembling 2D crystals. Generating a single domain 2D crystal has many applications from a negative refractive index to directionality varying band gaps, and di-electric constants[11-13].

These properties could lead to new advances in optical computers as well as materials that may be able to bend light around an object. Current research involves external control of the assembly of these particles by manipulating gravitational forces[14-15] as well as electric fields[16-17]. However we

believe that depletion forces in two dimensions can be useful in crystal formation that does not require as much intervention. Depletion interactions can be tuned to give kT scale interactions. Additionally, through the use of changing the size of depletents[1] and the interactions between depletents[9], we can change the length scale of the interaction as well as the interaction potential. In concert with applying patterned surfaces onto a substrate, this could be used to help generate crystals with fewer defects.[18]

We hope to develop a theory that is applicable to all two dimensional depletion interactions. Our approach to study depletion at a 2D interface was to first adapt the Asurka and Oowasa theory to two dimensions. To test the accuracy of this theory, we developed a two dimensional Monte Carlo simulation to simulate depletion interactions in a 2D system. We simulated two large particles in a sea of smaller depletants. We then confirmed the A.O. theory with these simulations. After that, we developed a more complicated depletion adsorption theory based on Lekkerkerker's adsorption theory[19]. We developed this as the A.O. theory could not predict the effects of depletant-depletant interactions on the depletion interaction. We then used our simulation to test this new theory and ensured our theory and simulations were in agreement at low concentrations of depletants. We then increased the depletant concentration to determine the point at which our predictions break down. We wanted to determine the effectiveness of our ability to predict the interaction potentials between the large particles at high concentrations. Additionally, we wanted to determine if the discrepancies between the observed and predicted potentials would affect the second viral coefficient of the colloids and the contact forces as these are important crystal formation parameters.

1.1 Simulation overview / Experimental methods

In order to test our theory on two dimensional depletion forces, we elected to use simulations for our experiments. Simulations allow for precisely defined interactions between particles, and are

not subject to environmental conditions. Additionally, there are no unknown interactions that we must account for. Finally, simulations are relatively easy to set up and gather data.

We elected to use a Monte Carlo simulation as opposed to a molecular dynamics simulation. A Monte Carlo simulation is easier to code and implement and we did not require any dynamic parameters such as diffusivity. We only required parameters that can be obtained at thermodynamic equilibrium.

Our Monte Carlo simulation was written in FORTAN , as that language is good at executing code efficiently[20]. We used a Monte-Carlo simulation as all of our theories are based on thermodynamic equilibrium. We used a NAT or constant number of particles, constant area (2D), and constant temperature ensemble. This fixes the area fraction of the depletants in the simulation. As this was a self-built code, we feel compelled to talk about its design and implementation to assure the reader that it was functioning properly.

Our Monte Carlo simulation works by first selecting an object at random within the simulation. Next, the simulation proposes a move for that object, which can either be accepted or rejected. The maximum length of this proposed move is tuned to give 20 percent move acceptance. If there are too many accepted moves, the step size will increase. Likewise if there are too many rejected moves, the step size will decrease. It is advisable to limit the maximum step size, especially when using speed improvements; or when simulating a very dilute system. The upper bound of the maximum step size is that of the simulation box.

The simulation functions as a Markov chain, and as such we must follow balance conditions to ensure that the simulation will reach thermodynamic equilibrium. However it is often easier to adhere to detailed balance conditions, a subset of balance conditions. Detailed balance conditions are:[21]

$$f_i * P_{ij} = f_j * P_{ji} \tag{1}$$

While adjusting the step size of a system while running does violate the detailed balance condition of a Markov chain, this does not invalidate the simulation results[22]. The tuning of the step size is necessary to achieve an efficient simulation, and changing the step size does not bias the system. After a particle is selected and a move is proposed, the change in energy for the system before the move and after the move is calculated. We then use the following algorithm to determine the move's acceptance.

$$
\begin{aligned}
&If\ \Delta u \le 0 \\
&\text{Then:} \\
&\text{Accept Move} \\
&\text{Else if}: UniformRV[0,1] < \exp(-\Delta u) \\
&\text{Then} \\
&\text{Accept Move} \\
&\text{Else:} \\
&\text{Reject Move}
\end{aligned}
\tag{2}
$$

This algorithm allows moves that are energetically unfavorable to occur as prescribed by the Boltzmann distribution. If all movements were required to be more energetically favorable, then the simulation would quickly reach an energy minimum and become frozen. Once the system has reached equilibrium, the amount of energy in the system remains relatively constant.

1.2 Periodic boundary conditions

Our simulation uses periodic boundary conditions to simulate a bulk region and eliminate edge effects[23]. Periodic boundary conditions are when the edge of one side of the simulation folds over to the other.

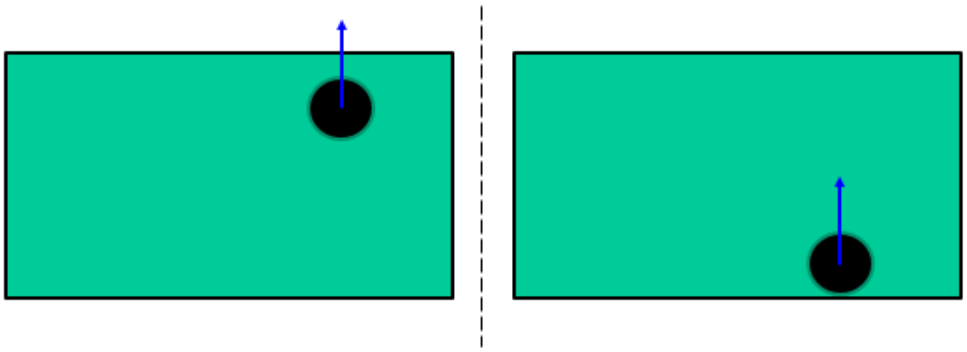

Figure 1-1: Periodic boundary conditions. The particle moves through the top edge of the simulation box to appear at the bottom of the simulation box.

If a particle is moving toward the edge of the boundary, it will appear on the other side of the simulation box. Additionally all interactions between objects in the simulation can be performed across this edge. When calculating the distance between particles, the closest path may be across the simulation boundaries. This allows a bulk fluid to be simulated, as there are effectively no boundaries in any direction.

1.3 Simulation initialization:

The FORTRAN code reads in all of the information needed from two start files. One file contains all of the parameters of the simulation such as the size of the simulation box, the number of particles, and the area fraction of the depletants. The second text file contains the initial positions of the colloids and the depletants. This allows us to keep the same base code for different simulations, but change the simulation parameters; lending our framework a great deal of flexibility.

1.4 Size ratio

We tested a variety of size ratios ranging from 2:1 to 50:1 to determine the optimal size ratio for our simulations. This gave us the additional benefit of ensuring that our theory and our simulations were correct; as we could predict the effect of changing the size ratio would have on the depletion potential.

We selected a colloid to depletant size ratio of 10:1 for investigating our system. We determined this was a good size ratio as there was a significant amount of depletion interaction predicted by the A.O. potential. One benefit of such a size ratio is it does not require as many macromolecules to simulate as a size ratio of 100:1. The number of depletants in simulation scales with the size ratio squared, so a size ratio of 100:1 would require 100 times more depletants than a 10:1 system. This allows the simulations to be run at a faster pace, and it allows for much more accurate data to be extracted from the simulation. A ratio of 10:1 is not an unrealistic size for a depletion interaction, and the interactions energies are on the order of kT; which allows for great tunability.

1.5 Efficiency improvements

Traditionally, when a move is proposed, the new particle position is compared to all of the particles within the simulation. The run time of calculating a particle's move will scale with n as a particle needs to be compared to all other n-1 particles. We define the run time to be the time it takes for the simulation to propose and evaluate n moves. Therefore, the total computation time for such a simulation scales with n^2. As we increase the size of the simulation, we will be able to extract less information per computing time.

There were a number of methods we used to increase the speed of the simulation. The first is the use of a mesh type algorithm. This splits the simulation space up into many boxes. When an energy is calculated, only the particles in the same box and surrounding boxes are considered. Particles outside of that area would only have extremely small contributions and can be neglected. As we have an exponential decay for our potential functions, we have a cutoff distance of $6a_d$ in our simulations.Beyond which the depletants energy contributions are negligible and not considered. Therefore we only need to calculate the energies within the 9 boxes that are closest to the particle, and not the entire simulation. This greatly reduces the number of comparisons that are required. The number of comparisons when a move is proposed does not

scale with n, but is now constant. This allows much larger simulations to be run as the simulation time will now scale with n.

This method has a few constraints that can limit its implementation. First, the sizes of these boxes cannot be less than the cutoff distance for the calculation of particle energies. This would bias the particles at the edge of the boxes. Additionally, if the simulation space is small, then there is not much incentive to implement a grid mesh algorithm. If the size of the simulation is only a few times larger than the cutoff distance, then only a few boxes exist, and most particles will be compared leading to a more complex simulation that is no faster.

Another computational time saving method was to restrict the large particles to movement in the X-direction only. This sped up the simulation as it caused the large particles to be closer together on average. This allows us to calculate a more accurate potential between them. Additionally, this allowed us to shrink the size of the simulation in the Y-direction. Doing this reduced the number of particles required for a specified area fraction. This allowed for the simulation to run quicker as the simulation speed scales with $1/n$.

Our cluster has 136 cores and they are mostly being unused. As opposed to running one long simulation, we would often run 10 simulations that were $1/10^{th}$ the number of steps. This would allow us to run our simulation quicker and split up the work amongst the cores. Each instance would have a different random seed for the random number generator, so the trajectories of the system would be different. This allowed us to gather 10 times the data in the same period of time.

Our final speed improvement was to specify the colloids to be selected at 10 times the rate of the depletants. We did this in order to prevent the colloids from becoming stuck. This allowed them to sample more space, which allowed for more frequent recordings of the distance between them. Note that since these particles start with, and maintain their increased selection rate, this does not violate detailed balance conditions.

Finally, to ensure that the system is at thermodynamic equilibrium, we ran the simulation for 100,000,000 steps before collecting any data. The equilibrium was then confirmed by plotting the total energy of the system versus step number.

1.6 Specifying number of colloids

Depletion potential simulations had two colloids, as this would allow us to study the depletion potential without multi colloid packing effects. With only two colloids, we can use the Boltzmann inversion of the radial distribution function outlined in the data extraction section as this is considered infinite dilution. If there were more colloids, we would not be able to make this assumption, as there can be multi-body forces that we would have to account for.

When we wanted to extract the density profile of depletants near a colloid, we used one large colloid, as a second large particle distorts the $g_{cd}(\mathrm{r})$. This is because there is a large void where no small particles can occupy. This void is difficult to account for and it is much simpler to eliminate the second colloid and simply run a simulation with a single colloid. This allows us to obtain an accurate density profile away from a colloid, which we will later use to compare to our predicted density profiles.

1.7 Specifying number of depletants

The X-direction length of the simulation box is fixed and then a target Y-direction length of the simulation box is set. Then the number of depletants required for the specified area fraction is calculated and rounded to the nearest whole integer. The area fraction will now be slightly over, or slightly under the target area fraction. The simulation will adjust the Y-direction height so the area fraction is as prescribed by the text file.

1.8 Data extraction

We extract three categories of information from the simulations. The first category is information of radial distribution functions, and this has three subcategories. The first subcategory is the radial distribution function between colloids $g_{cc}(\mathrm{r})$. This is easy to obtain as there are only two

particles. This is collected by establishing bins that are .05 a_d wide. Every 200 moves, the position is recorded and 1 is added to the bin of the corresponding particle separation. We chose .05 a_d as the bin width as it gives good resolution while also giving acceptable levels of noise. At the end of the simulation the values of the bins are written to a text file that is to be analyzed later in MATLAB. This subcategory is the reason that the simulation needs to be so quick and so efficient. When a g(r) is calculated in a simulation that has 100 depletants; then for each round of recording, there can be (99*100)/2 positions recorded. The number of data points in computing a g(r) scales with n^2 . However when one is recording the positions of 2 particles, there is 1 piece of information. In the same number of simulation steps, a simulation that has 100 particles will gather 4950 times the radial distribution data then a simulation that has 2 particles. Because of this inherent inefficiency, we ran 10 billion steps per simulation.

The second type of radial distribution function obtained is the $g_{cd}(\mathrm{r})$. This radial distribution function describes how the depletants are distributed around the colloids. This radial distribution function is obtained from simulations that have only one colloid. If there were two colloids, then the second colloid would affect the radial distribution function, and it would skew the results. For every round of recording in a 100 depletant simulation, you would get 100 data points to add to the radial distribution function.

The third type of radial distribution function is $g_{dd}(\mathrm{r})$. This requires the fewest number of simulation steps as it is possible to collect $n(n-1)/2$ points per round of particle moves. This is typically used for studying bulk systems to determine packing effects, second viral coefficients, etc.

The second type of data that we extracted from the simulations was information about the particles absolute positions, and here there are two sub categories. The first subcategory was the

output of the particles' exact positions to a text file every 100,000 steps. This was done so that we could make movies of the particles to observe their motion. These text files are very large, so we opted to limit this to only 1000 frames per simulation. These positions were recorded after the initial equilibrium stage to give good bulk movies.

The second subcategory of particle information was for the creation of heatmaps. We created a grid over the entire simulation space with a resolution of 0.1 a_d and every 1000 steps, we added 1 to the box whenever there was a depletant center in that box. The colloids were held at fixed positions for these simulations. At the end of the simulation, FORTRAN wrote a text tile containing the grid values. We then used MATLAB to read in the text files and analyze them to generate heatmaps. We used this information to determine the validity of the superposition principal of depletant profiles.

The final category is used to ensure that the simulation is working properly. These text files record the step size of the simulation, the area fraction, the total energy of the simulation.

1.9 Calculating potentials from simulations

Our theory compares the interaction energy between the large particles, however our simulation does not output the interaction potential between them. We can calculate the interaction potential between them as we know how often they sample certain positions. We use a Boltzmann inversion to accomplish this. The equation is:

$$-\ln\left(g_{cc}(h)\right) = \frac{u_{cc}(h)}{kT} \tag{3}$$

However it helps to have some background on where that comes from. Here we define state i to be some specified particle separation and state ref to be the reference state. We define state ref as having zero energy [24].

$$\frac{N_i}{N_{ref}} = \frac{g_i}{g_{ref}} \frac{\exp(-u_i / kT)}{\exp(-u_{ref} / kT)} \tag{4}$$

Degeneracy g is defined as the possible number of microstates at a particular separation. As our large particles are confined to the X-axis only, the degeneracy of any possible separation are equivalent as the bins are the same width.

$$\frac{N_i}{N_{ref}} = \exp(-(\mathrm{u}_i)/\mathrm{kT}) \tag{5}$$

$$-\ln\left(\frac{N_i}{N_{ref}}\right) = \frac{u_i}{kT} \tag{6}$$

Because we recorded the number of times particles were in each bin, we can determine the energy of each bin, if we have a reference state. Normally we would select infinite separation as the zero of energy, however an infinite distance in a polynomial time simulation is not feasible. To calculate a reference state, we calculate the reference state to be furthest quarter of the bins obtained in the $g_{cc}(\mathrm{h})$. These bins have a constant value and only differ by random noise. By averaging these bins, we are able to obtain an accurate reference state.

1.10 Defining area fraction

Since our depletion potentials are dependent on area fraction, any simulations must be run at the correct area fraction. It is possible for some ambiguity in this definition. To answer how to properly define area fraction we will turn to a thought experiment:

Suppose that there exists a simulation within a square that has periodic boundary conditions with total area A. If we compare that to a square that does not have periodic boundary conditions, but still has total area A, the particles in the simulation with periodic boundary conditions undoubtedly have more accessible area available to them; but both have area A.

A second thought experiment is to have two separate simulation squares, both with periodic boundary conditions and area A. The first square has an infinitely small point that has negligible area, but hard wall interactions with all particles. This impedance has no effect on the area A, but

it confines the particles and restricts their movement. The second square has no such point particle and has no impedances.

One possible solution to these problems arises if we look at the center accessible area, or more precisely "the area accessible to the center of the depletants." [25] We can test this hypothesis with our simulation system and the theory we have developed for ideal depletants. We found that the center accessible area methodology was the proper method to calculate the area fraction of the system. This would explain the differences in areas in each of the thought experiments. For our system, we use the following equation to calculate area fraction:

$$\eta = \frac{(X_{length} * Y_{length} - \pi * \#Colloids(\mathrm{a}_d + \mathrm{a}_c)^2)}{\#\text{Depletants} * \pi a_d^2} \tag{7}$$

1.11 Reducing the number of system parameters

In order to reduce the number of system parameters, we can make a dimensionless distance and dimensionless colloid size. By scaling all lengths by a_d we can reduce the number of variables required to predict the A.O theory. This necessarily sets the standard unit of length to one depletant radii for the system. This has the effect of changing sizes relative to the size of the depletant. For example the large particles are not judged by their absolute size, but rather relative to that of the depletant. From this we learn that the absolute size of the depletants and particles does not matter for interaction potentials, but rather it is the size ratio that is important. (Appendix 2)

1.12 Depletant-depletant interactions

The purpose of this thesis is to determine how varying depletant-depletant interactions will affect the depletion force between the larger particles. As they form the focus of the thesis, we will review them now and how they are applied to the simulation. We use three types of depletant-deplant interactions in this thesis.

1.12.1 Ideal depletant interactions

The first simulations we ran were with two large particles, and approximately 100 smaller depletants. We specified hard disk interactions between the colloids, hard disk interactions between the colloids and the depletants, and no interactions between the depletants.

$$\begin{aligned} u_{cc}(\mathrm{h}) &= \begin{matrix} 0\, if\ h > 0 \\ \infty\, if\ h \le 0 \end{matrix} \\ u_{cd}(\mathrm{h}) &= \begin{matrix} 0\, if\ h > 0 \\ \infty\, if\ h \le 0 \end{matrix} \\ u_{dd} &= 0 \end{aligned} \tag{8}$$

These ideal depletant-depletant also allow us to perfectly describe the osmotic pressure of the depletants in the system:

$$\Pi = \rho kT \tag{9}$$

Not having any depletant-depletant interactions allows the A.O. theory to be tested and confirmed in an ideal environment. Because these depletants do not influence each other, they do not have any packing effects that can affect their particle-depletant distribution functions. Such limiting cases are important to test as it helps determine if the simulation is functioning properly. These cases also help firm up our beliefs of the theory we developed.

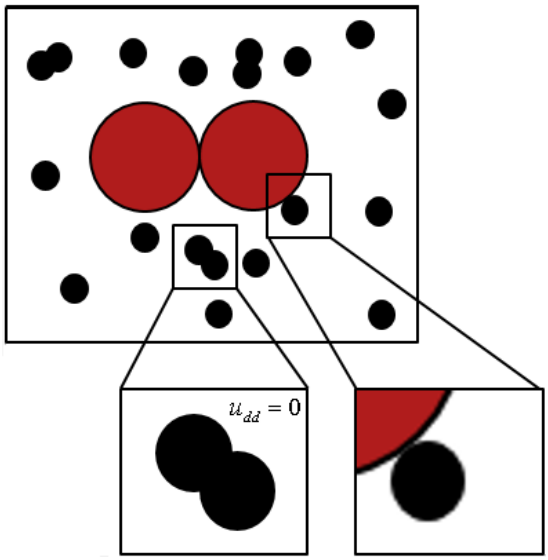

Figure 1-2: Visual representation of ideal depletants in simulation. Depletants are allowed to pass through each other and have no interaction. Depletants still retain hard wall interactions with colloids

After we confirmed our theories with ideal depletants, we wanted to add complexity to the system and determine if we were still able to accurately predict the depletion potential. The next logical step was to add hard disk interactions between depletants. Adding these interactions would change the depletant density profile near a colloid, which would alter the depletion interaction between colloids.

1.12.2 Hard disk depletants

Hard disk interactions are common in simulations as they have a very low calculation time. This is very important as the computation time to compute a Van der Walls interaction versus an if-statement can be orders of magnitude less. The mathematical simplicity led to hard disk interactions being the de-facto starting point with any simulation. This was of great significance to scientists creating the first simulations as it allowed for fast computation times as they had very limited system resources. One of the earliest discoveries of simulations was a phase transition to a liquid at high volume fractions using only hard disk interactions[26]. It was previously thought that this was impossible and that entropy would prevent this from happening. The idea that a crystal could form without any attractive interactions between particles seemed counterintuitive.

We are applying it here as there is previous research into the effect of hard disk interaction on the depletion force between two large objects. This gives us a method to test the validity of the results we get from our simulations. The equations that govern this system are:

$$u_{cc}(\mathrm{h}) = \begin{matrix} 0\, if\ h > 0 \\ \infty\, if\ h \le 0 \end{matrix}$$
$$u_{cd}(\mathrm{h}) = \begin{matrix} 0\, if\ h > 0 \\ \infty\, if\ h \le 0 \end{matrix} \qquad (10)$$
$$u_{dd}(h) = \begin{matrix} 0\, if\ h > 0 \\ \infty\, if\ h \le 0 \end{matrix}$$

1.12.3 Attractive depletants

As we wanted to determine the effect of Van der Walls interactions between depletants on the depletion force we need to define the interactions between the depletants. As computing an exact Van der Walls potential can be computationally intensive, we selected an alternative potential that was qualitatively similar to a Van der Walls interaction. The original potential for Au-np's at an oil-toluene interface was:[27]

$$u_{dd}(\mathrm{h}) = \frac{5.958*10^{-4}*(h)^3 - 2.844*(h)^2 + 670.2*(h) - 7029}{(\mathrm{h})^3 + 1674*(h)^2 + 1934*(h) - 13.96} kT \qquad (11)$$

(Where h is in units of nano-meters)

With a shifting hard wall to control for contact values of attraction. This has the problem of changing the size of the depletants, which we want to remain constant. Additionally, by changing the size of the depletant, it would change the size ratio between the colloid and the depletant. Since a_d is changing, we would have to re-calculate the area fraction. As the standard unit length is a_d , this would change the length over which the potential acts. Finally the profile does not retain the same shape over many different values of contact energy. For these reasons, we decided to keep the hard wall at the same place, and institute an approximate method for calculating the interaction between the two particles. This can be altered for a variety of

interactions. The interactions could be made to occur over a longer or shorter range, or decay in a different manner.

$$u_{dd}(\mathrm{h}) = \alpha \exp\left(\frac{-2\,\mathrm{h}}{kT}\right) \tag{12}$$

We chose this form as it decays quickly, is easy to calculate, and is qualitatively similar to the Van der Walls interaction between Au-np's. (11). To vary the amount of attraction, the constant α can be changed. One benefit of this form of attraction is that the decay length is very short. This allows us to create smaller boxes in the simulation which allows for a quicker simulation.

2 Theory

Now that we have discussed our experimental methods we will discuss how we will apply these methods to create a useful understanding of two dimensional depletion. We will start with the 3D A.O theory and change it to accommodate two dimensions. Then we progress to an adsorption-depletion theory by Lekkerkerker and see that it reduces to the A.O case when we have ideal depletants. Next, we want to extend this theory to non-ideal depletant-depletant interactions. To achieve this, we will take cues from Glandt and Walz on how to calculate depletant density profiles around a colloid.

2.1 Asurka and Ooswasa theory

The Asurka and Ooswasa theory can be derived in a number of ways, which yield the same analytical result. The theory supposes two flat plates, both of area A, immersed in a fluid of non-adsorbing, mono-dispersed polymer. In this simplified model, there are hard wall plate-plate interactions, depletant- plate interactions but no depletant-depletant interactions. As the plates approach each other, the gap between the plates becomes too small for the depletants to occupy. This caused an osmotic pressure difference between the medial side of the plates and the distal side of the plates. This generates a net force that pushes the plates toward each other.

2.1.1 Three dimensional idealized depletion

Since the force between plates is constant in the A.O. theory, it is easy to integrate the force to obtain a potential function of distance between the plates[6].

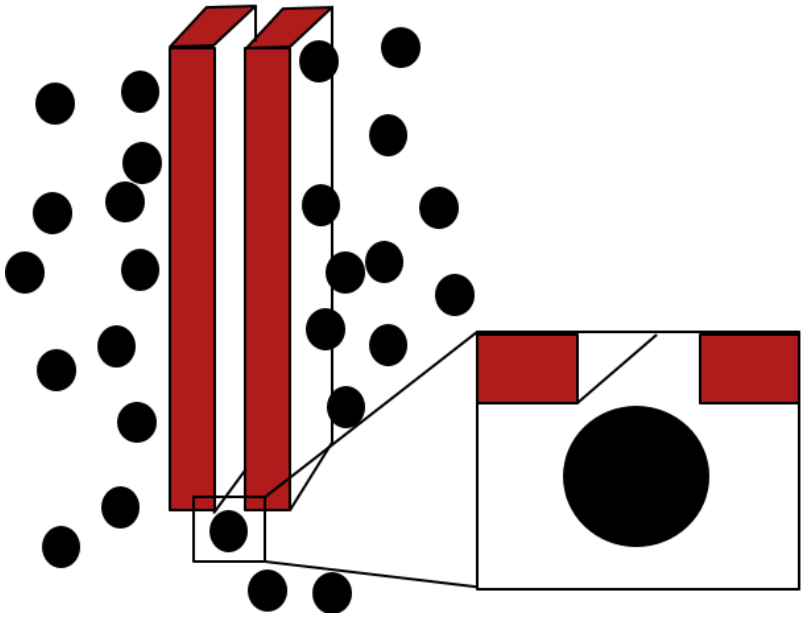

Figure 2-1:Pictoral representation of A.O. theory. Two large plates are closer than the diameter of depletants which causes a net osmotic pressure differential between the inside walls of the plates and the outside walls of the plates

$$\frac{F_{cc}(\mathrm{h})}{Area} = \begin{matrix} \Pi \; if \; h \le 2a_d \\ 0 \; if \; h > 2a_d \end{matrix} \tag{13}$$

$$u_{cc}(\mathrm{h}) = \int_0^\infty F_{cc}(\mathrm{h})\,\mathrm{dh} \tag{14}$$

$$\frac{u_{cc}(\mathrm{h})}{Area} = \Pi(\mathrm{h} - 2\,\mathrm{a}_d) \tag{15}$$

We can cast this in a different format if we so choose. Because osmotic pressure is an entropic force, we can think of the A.O framework as a special case of the depletion force. We notice that as the plates approach each other, the center of the particles gain access to a larger volume.

Imagine a series of infinitely thin plates confined to the X-direction: As the depletants want to increase the volume accessible to them they will force the plates together. As these plates are

infinitely thin, they will end up stacked directly on each other, as this confirmation is the most entropically favorable for the system.

We can recast (15) in terms of the change in center accesable volume, allowing us to investigate other shapes besides flat plates.

$$\frac{\Delta V}{Area} = (h - 2a_d) \tag{16}$$

$$\frac{u_{cc}(h)}{Area} = \Pi * \Delta V \tag{17}$$

Plates are not the only geometry that can have an excluded volume overlap. When two large spheres are placed close to each other in a simulation, the amount of volume accessable to depletants increses. We can represent this volume increase as[28]:

$$\Delta V(h) = \frac{\pi}{12}\left(6a_c + 4a_d + h\right)\left(2a_d - h\right)^2 \tag{18}$$

2.1.2 Two dimenstional idealized depletion

Up until this point, we have only considered the depletion interaction in three dimensions. However we want to investigate how depletion forces effect 2D crystal growth and formation. We will now shift our focus from the original 3D framework of the A.O. and adopt it for two dimensions. If we considered a 2D plane instead of a 3D space, the definitions of the units of force and energy change. To ease understanding, we are keeping the colloquial terms of "pressure" and keeping the term Π .Instead of calculating the force in terms of unit area for plates, it will now be calculated in force per unit length for lines. This is the projection of the plates on to a 2D surface. Additionally, the center accessible volume will become center accessible area. The potential energy of two lines on a plane becomes:

$$u_{cc}(h) = -\Delta A \Pi \tag{19}$$

Similar to spheres in 3D, disks that are comparatively large experience depletion forces .

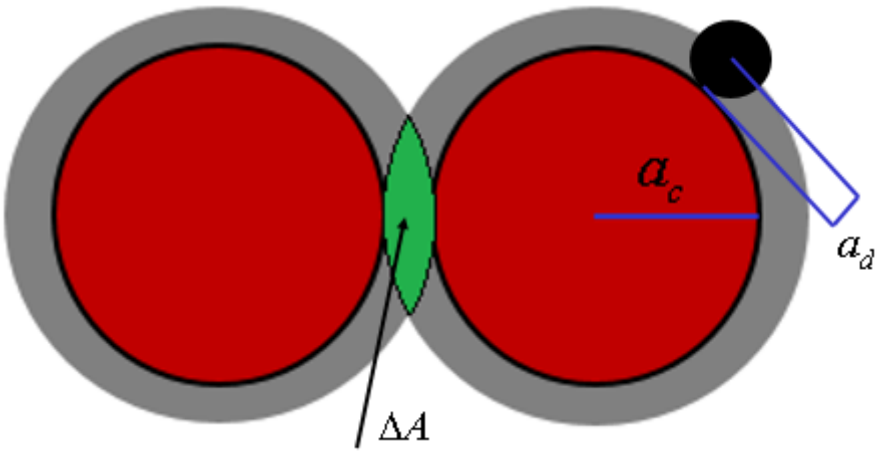

Figure 2-2: Demonstration of change in excluded area as colloids approach each other

As the disks approach each other, their center excluded areas overlap. This has the effect of increasing the total area available to depletants. This increase in area to depletants is entropically favorable. A different and more rigorous derivation method is available (Appendix A), however these different methods ultimately result in the same equation[29].

$$\Delta A(\mathrm{h}) = \begin{array}{l} if\ h \le 2a_d \\ if\ h > 2a_d \end{array} \begin{array}{l} \left(2\left(a_d + a_c\right)^2 \cos^{-1}\left(\frac{h + 2a_p}{2\left(a_c + a_d\right)} \right) - \frac{\left(h + 2a_c\right)}{2} \sqrt{4\left(a_c + a_d\right)^2 - \left(h + 2a_c\right)^2} \right) \\ 0 \end{array} \tag{20}$$

$$u_{cc}(\mathrm{h}) = \begin{array}{l} if\ h \le 2a_d\ \Pi \\ if\ h\ > 2a_d \end{array} \begin{array}{l} \left(2\left(a_d + a_c\right)^2 \cos^{-1}\left(\frac{h + 2a_p}{2\left(a_c + a_d\right)} \right) - \frac{\left(h + 2a_c\right)}{2} \sqrt{4\left(a_c + a_d\right)^2 - \left(h + 2a_c\right)^2} \right) \\ 0 \end{array} \tag{21}$$

Using a particle simulation we have confirmed this theory to be true, and We can successfully predict the depletion potentials for different area fractions as well as size ratios. (Figure 3-1, Figure 3-2) However, the results of this simulation only test the limiting case of ideal interactions. When we add interactions to the depletants in our simulation, the potential curves no longer

match up to the A.O theory. The A.O theory cannot predict this behavior, and as such, we turn to another framework; adsorption, to predict this behavior.

2.2 Adsorption theory

By measuring the number of depletants that are adsorbed around the colloids as a function of separation, we are able to determine the interaction potential between the colloids using adsorption theory[19]. Here we define adsorption as depletants adsorbing to colloids. We draw a box around two large particles, and imagine that box is in contact with an infinite depletant sink at the same bulk concentration. We can measure the adsorption as the number of depletants that enter the box. This would work with any arbitrary shape, provided that the boundaries are sufficiently far away from the colloids as to be at bulk concentration. We chose a square, as it is the easiest shape to demonstrate, and its integration is simple. Below are the generalized equations for predicting the interaction energy between colloids[19].

$$u_{cc}(\mathrm{h}) = \int_0^{\rho_b} \left[\Gamma\left(\infty, \rho_b^{'}\right) - \Gamma\left(h, \rho_b^{'}\right)\right]\left(\frac{\partial \Pi}{\rho_b^{'} * \partial \rho_b^{'}}\right) d\rho_b^{'} \tag{22}$$

$$\Gamma\left(h, \rho_b\right) = \int_{-xbound}^{xbound} \int_{-ybound}^{ybound} \left[\rho\left(x, \mathrm{y}\right) - \rho_b\right] dxdy \tag{23}$$

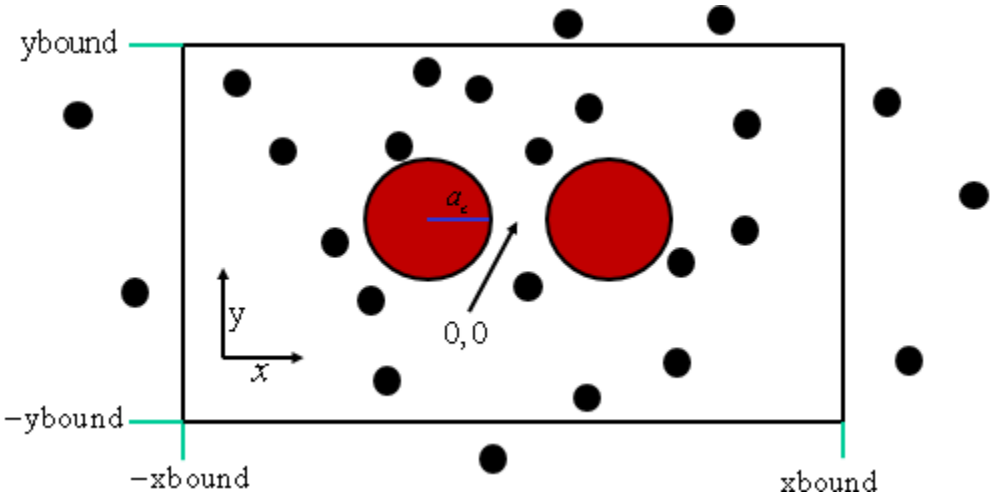

Figure 2-3: Arbitrary box defined for the purposes of defining adsorption. The edges of the box are sufficiently far from the colloids to be kept at bulk concentration. The box is surrounded on all sides by an infinite sink of depletants at the same area fraction.

Where predicting the depletant density profile $\rho(\mathrm{x},\mathrm{y})$ is done using either superposition of the Glandt derived profile, or superposition of the depletant density profiles obtained from a simulation with one particle. When calculating $\left(\frac{\partial\Pi}{\rho_b^{'} * \partial\rho_b^{'}}\right)$ we used perturbation theory about a hard disk system to calculate the change in osmotic pressure with respect to ρ [30-31].

$$\Pi = \Pi_{HD} + \rho_b^2 kT\pi \int_{2a_d}^{\infty} g_{dd}(\mathrm{r}) \frac{u_{dd}(\mathrm{r})}{kT} r dr \tag{24}$$

$$\Pi_{HD} = \rho \frac{\left(1+\frac{\eta^2}{8}\right)}{(1-\eta)^2} \tag{25}$$

2.2.1 Two dimensional idealized depletant adsorption

To calculate adsorption for disks, we need to make some geometric manipulations. We first start by defining two new coordinates for simplicity: r_1 *and* r_2. They describe the distances to the center of the two colloids from any point in the X,Y plane.

$$\rho(\mathrm{x},\mathrm{y}) = \begin{matrix} \rho_b \; if \; r_1 \geq (a_c + a_d) \;\; \& \;\; r_2 \geq (a_c + a_d) \\ 0 \quad Otherwise \end{matrix} \tag{26}$$

$$\begin{aligned} r_1 &= \sqrt{y^2 + \left(x + \left[a_c + \frac{h}{2} \right] \right)^2} \\ r_2 &= \sqrt{y^2 + \left(x - \left[a_c + \frac{h}{2} \right] \right)^2} \end{aligned} \tag{27}$$

Where the X-bound and the Y-bound are the edge of the box where there exists a sink at the same chemical potential. They can be defined as infinity, for the purposes of integration.

Upon integration of Γ , the adsorption can be described as:

$$\Gamma(\rho_b, h) = \begin{matrix} \rho_b \left(2(a_d + a_c)^2 * \cos^{-1}\left(\frac{h + 2a_c}{2(a_c + a_d)} \right) - \frac{(\mathrm{h} + 2a_c)}{2} \sqrt{4(a_c + a_d)^2 - (\mathrm{h} + 2a_c)^2} \right) if \; h \leq 2a_d \\ 0 \; if \; h > 2a_d \end{matrix} \tag{28}$$

Upon plugging this into (22) we recover the A.O. potential of :

$$\mathrm{u}_{cc}(\mathrm{h}) = \begin{matrix} \rho_b kT \left(2(a_d + a_c)^2 * \cos^{-1}\left(\frac{h + 2a_c}{2(a_c + a_d)} \right) - \frac{(\mathrm{h} + 2a_c)}{2} \sqrt{4(a_c + a_d)^2 - (\mathrm{h} + 2a_c)^2} \right) if \; h \leq 2a_d \\ 0 \; if \; h > 2a_d \end{matrix} \tag{29}$$

This shows us that the adsorption theory agrees in the limit of ideal depletants, which gives us confidence in the theory as we progress forward.

2.2.2 Predicting depletant density profiles

However, this is only with an idealized version of the density function. Glandt et al. have developed a theory to predict particle densities away from a wall. [8-9]

$$\rho(\mathrm{h}) = \rho_b \exp\left(\frac{-u_{cd}(\mathrm{h})}{kT} \right) * \left[1 + \rho_b \beta_2(\mathrm{h}) + O(\rho_b^2) \right] \tag{30}$$

$$\beta_2(\mathrm{h}) = \int_0^{\infty}\int_0^{2\pi}\left(\left\{\exp\left[\frac{-u_{cd}(\mathrm{r},\theta)}{kT}\right]-1\right\}\left\{\exp\left[\frac{-u_{dd}(\mathrm{r})}{kT}\right]-1\right\}\right)d\theta dr \qquad (31)$$

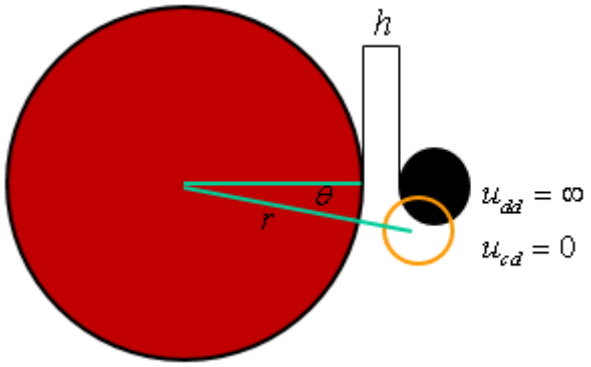

Figure 2-4:Illustritation of variables used to integrate Equation(31).

To test this theory, we constructed a simulation with one large disk and many small depletants. We only used one large particle to avoid any non-additive effects that depletant packing may cause when two large particles are simulated. This allowed us to test our predicted profiles against empirical profiles.

2.2.3 Superposition principle

As we saw some deviations in our density profiles from what we predicted, we decided to determine if the superposition of the observed density profile from the 1 particle simulation would approximate the depletant density of a two particle system. Additionally we wanted to know how well superimposing the Glandt theory would approximate the depletant density of a two particle system.

In order to determine if the superposition of the profiles is valid, we constructed heatmaps of the density around particles. We ran simulations with the positions of the colloids fixed and recorded the positions of depletants at intervals. This allows us to have a 2D map of the depletant density and determine if there is good agreement between our methods of prediction and the simulation.

2.3 Colloid-colloid second viral coefficient

In order to understand how multiple colloids interact, we look into how area fraction and the depletant-depletant interactions effect the colloid-colloid second viral coefficient. The second viral coefficient is important to the thermodynamics of crystal formation and it is used to understand crystal stability. We calculate the second viral coefficient using the equation[21]:

$$\beta_{cc} = -\pi \int_{2a_d}^{\infty} \left(\exp\left(\frac{u_{cc}(\mathrm{r})}{kT} \right) - 1 \right) r dr \tag{32}$$

Which we derived from the three dimensional derivation for the second viral coefficient. (Appendix 3) We want to determine if the differences between observed and predicted potentials seen at high area fractions will affect the second viral coefficients.

2.4 Contact force

One aspect of bulk behavior of colloidal flocculation is contact force. The force at describes the tendancy of a colloid to remain stuck to another colloid. If contact forces are too high, this can cause imperfections in crystals as they do not have enough thermal energy to correct imperfections. We measure this force by taking the derivative the derivative of the interaction energy at contact numerically by determining the slope of the last two points.

$$\frac{\partial u_{cc}(\mathrm{h})}{\partial h} = F_{cc}(\mathrm{h}) \tag{33}$$

The units of this derivative are in kT / a_d . If we dimensionalize these units, the contact force will scale with $1/a_d$. For this thesis, we specified a depletant size of 3.5nm as that is the size of the nanoparticles that started this work.

3 Results and discussion

With ideal depletants, we are able to exactly predict the outcomes of the simulation using the A.O. theory. This means we were able to correctly convert the 3D theory into a 2D theory.

Next we show the ability of our theory to predict what happens when we introduce hard wall interactions between depletants. At low area fractions, we are able to do this quite well, however as packing effects increase, our ability to predict these deviations decreases. After this we introduce attraction between depletants. At low area fractions and at low to moderate attraction we are able to predict the results quite well, however as we increase the area fraction, our predictions start to deviate. We discuss a few methods to curtail these deviations such as using the depletent density profiles from one colloid simulations to predict the density profile of a two colloid simulation.

Finally, we discuss how attraction lowers the second virial coefficient and the contact force of colloid-colloid interactions. This makes the depletion force an attractive option for creating self-assembled 2D crystals.

3.1 Ideal depletant results

When we ran simulations with ideal depletants, we could exactly predict the interaction energies of the colloids at all area fractions and at all size ratios. There is no breakdown of the density profile or of the energy profile. Both are exactly as described for all simulations that we ran.

3.1.1 Varying size ratio

To test the A.O. theory, we decided to run simulations at a variety of size ratios to determine its ability to predict interaction energy. The equations for the A.O. theory state that there is no dependence on absolute size, but rather the size ratio between the depletants and the colloids. This derivation is shown in (Appendix 2).

$$let:\ h' = \frac{h}{a_d}\ ,\ a_c' = \frac{a_c}{a_d} \tag{34}$$

$$u_{cc}(\mathrm{h}) = \begin{cases} if\ h \le 2a_d & \frac{\rho_b}{\pi}\left(2\left(a_c^{'}+1\right)\cos^{-1}\left(\frac{h^{'}+2a_c^{'}}{2\left(a_c^{'}+1\right)}\right)-\frac{\left(h^{'}+2a_c^{'}\right)}{2}\sqrt{4\left(a_c^{'}+1\right)^2-\left(h^{'}+1\right)^2}\right) \\ if\ h > 2a_d & 0 \end{cases} \quad (35)$$

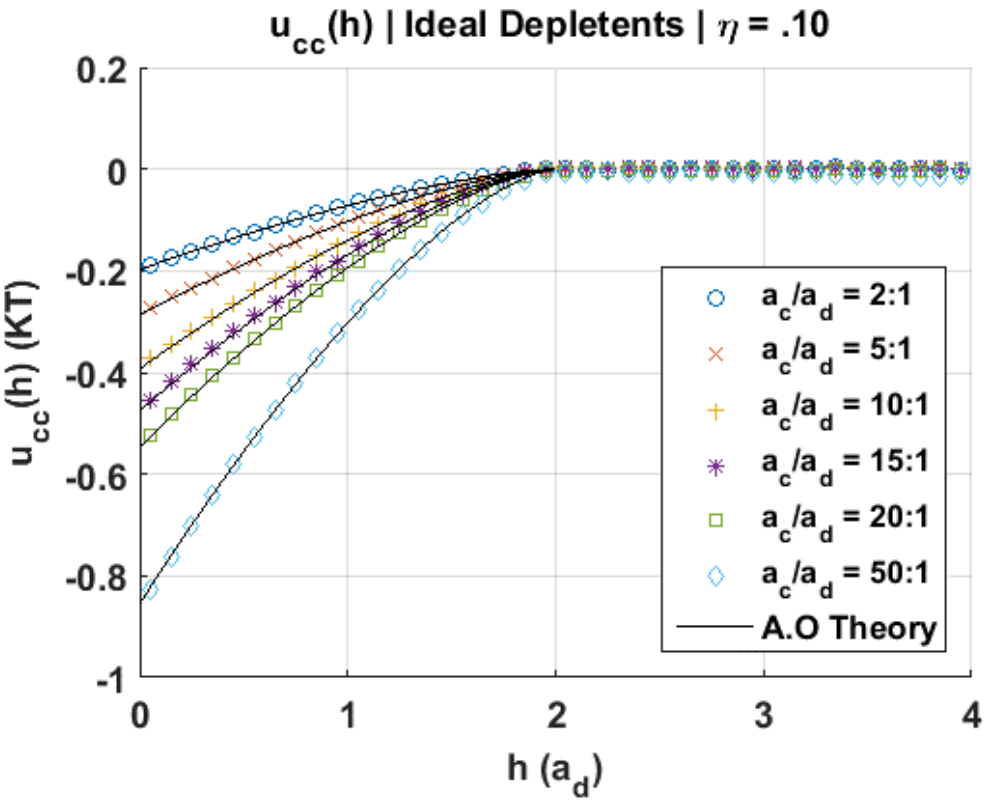

Figure 3-1: Colloid-colloid interaction potential with ideal depletants. η *=0.1 with varying size ratio. Black line represents A.O. theory.*

Here, we have perfect agreement between the results of our simulation and the predicted interaction potentials described by the A.O. theory and adsorption theory. This result allows us to be confident in both our simulation and our theory. We elected to perform the remainder of the experiments with a size ratio of 10:1 as it will allow us to keep a small simulation box while providing a nice size disparity.

3.1.2 Varying area fraction

Upon varying area fraction we were able to verify that our simulation experiments agreed exactly with the A.O. theory and adsorption theory. This bolstered our confidence in both our theory and our simulation as we feel confident that we can introduce depletant-depletant interactions.

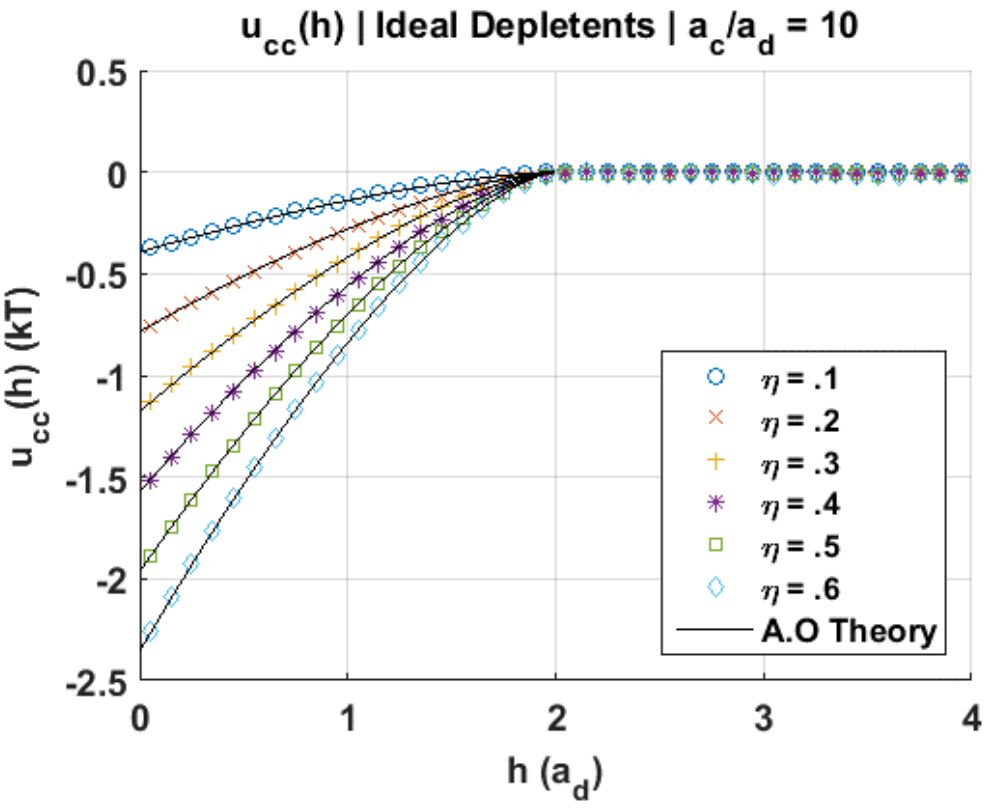

Figure 3-2: Colloid-colloid interaction potential with Ideal depletants. a_c / a_d *= 10 with varying area fraction. Black line represents A.O. theory.*

3.1.3 Adsorption theory with ideal depletants

In the case of ideal depletants, when the colloids get within $2\,a_d$ of each other, their excluded area overlaps. As the rest of the system is kept at bulk density, and the area available to the depletants increases, the number of depletants in the system increases by $\rho\Delta A$. This yields an energy of $u_{cc}(\mathrm{h}) = \Pi\Delta A$, which is the A.O. theory predicts.

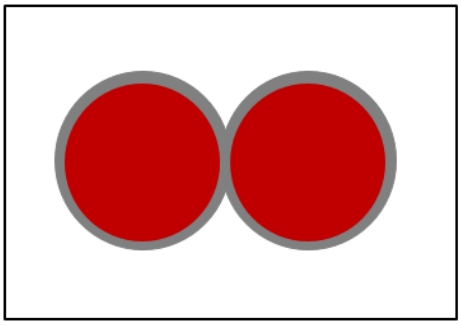

Figure 3-3: Pictoral representation of how overlap of excluded area (grey) increases the total amount of depletants in the system (Adsorption Theory)

3.2 Hard disk depletant results

Adding depletant-depletant interactions of any kind will introduce non-idealities into a system. In an attempt to reduce the number of degrees of freedom in describing a system, we lose some accuracy. However in doing so we are able to capture the majority of the interactions that give rise to depletion forces. As there are no intra-depletant forces other than the hard wall interactions, we would expect to be able to predict this system the best.

3.2.1 Depletant density profile prediction: Hard disks

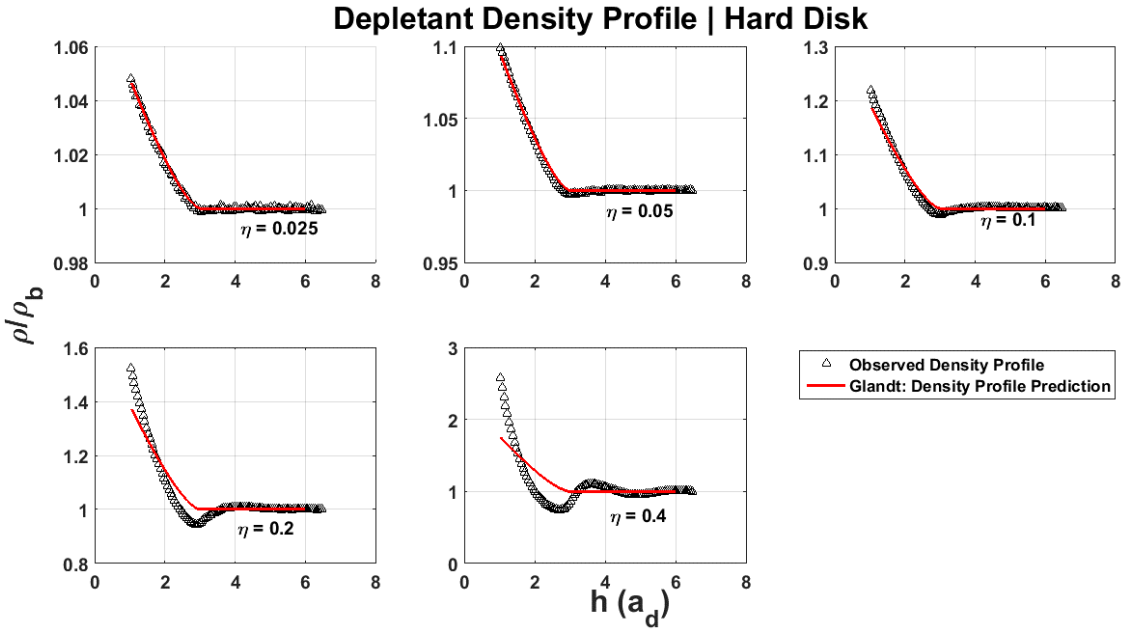

Figure 3-4: Distribution of depletants around colloid. Hard disk depetants. Red: profile predicted by Glandt's theory. Black: density profile observed in one particle simulation. Upper left: η = 0.025, Upper middle: η = 0.05, Upper right: η = 0.1, Lower left: = η 0.2, Lower middle: η = 0.4.

Using the machinery developed by Glandt et al. we were able to predict the depletant density near a colloid. At η of .025 and .05, we see that the simulation agrees almost exactly with our predictions. However as we increase η to .10, .20 and .40 we start to see deviations. The deviations appear to be oscillatory in nature, and we suspect they are related to packing effects. From the density profiles above we see that the depletants prefer to be closer to the colloid than part of the bulk. This has been observed in other papers in three dimensions with the density profile of hard spheres increasing closer to a wall[9]. As we are plotting ρ / ρ_b, we would expect the deviations on this graph to scale with ρ, as the non-ideal interactions should increase with ρ^2 for pairwise interactions.

3.2.2 Depletant density profile superposition

Glandt et al. derived the equations to predict depletant density profiles next to an object. However if we want to calculate the density next to two objects, we must superimpose the density profiles of the separate objects. We are uncertain of the accuracy of this superposition principle as there may be non-additive interactions. Additionally, we wanted to superimpose the depletant density profiles obtained from a simulation with one particle. To determine the validity of profile superposition we ran a simulation with two colloids fixed at specified positions in a sea of depletants. This allows us to determine if there are any non-additive effects as we can determine the two dimensional depletant density.

As we expect any deviations to be most pronounced at the highest area fractions, we will compare our predictions and observations of the density profile at $\eta = 0.4$. This high area fraction will highlight any deviations in the superposition principle. However, we also want to determine if the superposition principle works at more moderate concentrations such as $\eta = 0.1$. Therefore we will discuss the additivity of these two cases. Any non-additive effects would be far more apparent when the colloids are close, so we elected to plot the density profiles at $h = 3a_d$.

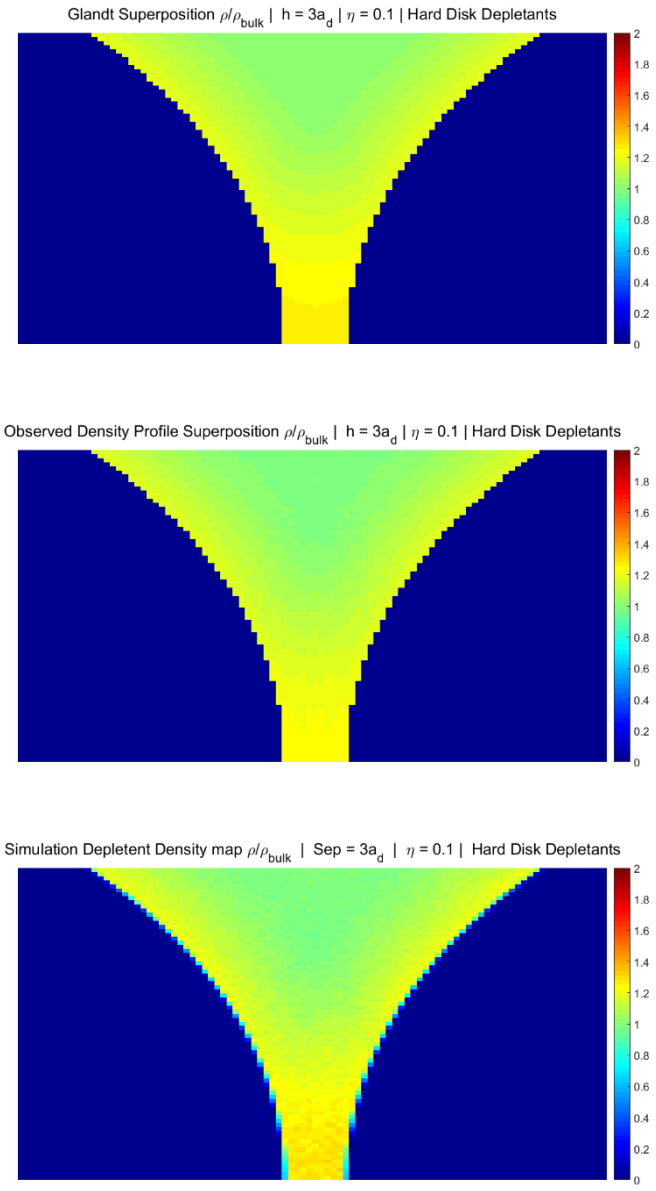

Figure 3-5: Heatmap of depletant densities with separation of 3 depletant radii and η = 0.1. Red = 2 ρ_b , Blue = 0 ρ_b , TOP: Superposition of Glandt theoretical density profiles. MIDDLE: :Superposition of observed density profiles around a single particle. BOTTOM: Heatmap obtained from simulation with two stationary particles.

While the density profiles are not very pronounced above, we can see that both of our attempts to predict the simulation's density map were successful. We feel confident that at low area fractions, the superposition principle is sufficient to predict depletant density profiles.

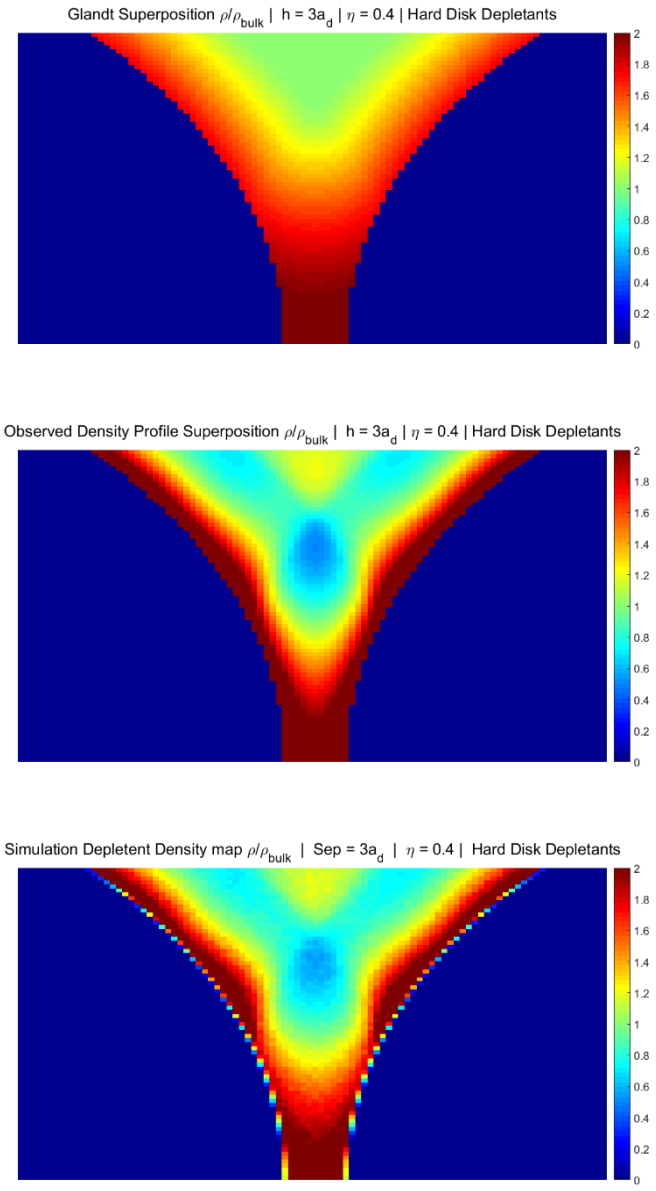

Figure 3-6: Heatmap of depletant densities with separation of 3 depletant radii and η = 0.4 Red = 2 ρ_b , Blue = 0 ρ_b , TOP: Superposition of Glandt theoretical density profiles. MIDDLE: :Superposition of observed density profiles around a single particle. BOTTOM: Heatmap obtained from simulation with two stationary particles. .

As we increase the area fraction, we see that the Glandt theory breaks down. However the superposition of 1 particle density profiles does a good job of predicting the density profiles. There are some minor deviations, however they are not very significant.

Our next goal is to take these 2 dimensional predicted density profiles and turn them into an adsorption profile. The total amount of adsorbed depletents will only change when the excess density profile intersects the excluded area of the other colloid.

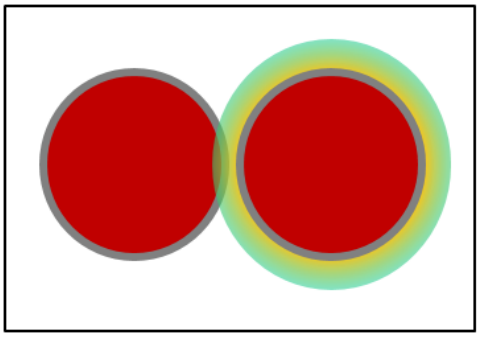

Figure 3-7: Demonstrating adsorption. The overlap of the center excluded area (red and grey) with the other colloids excess density profile, causes a net loss of particles inside the box for the hard disk case. The area overlapping with the excluded area has a higher density than that of bulk, causing a net migration of particles into the box

As the colloids move closer together, the edge of the excess density profile overlaps with the other colloids excluded area. This area of increased depletant density is effectively replaced by the same area at bulk concentration in the same way that the excluded area in the A.O. theory is replaced by bulk density. In this case we are replacing a greater concentration with a lower concentration, so there is a net desorption from our system. To visualize this desorption, we will look at depletent density profile maps generated from simulations. In these simulations we kept the colloids at a fixed distance and recorded depletents positions. We did this at colloid separations of 8,4,3,2,1,and 0 a_d.

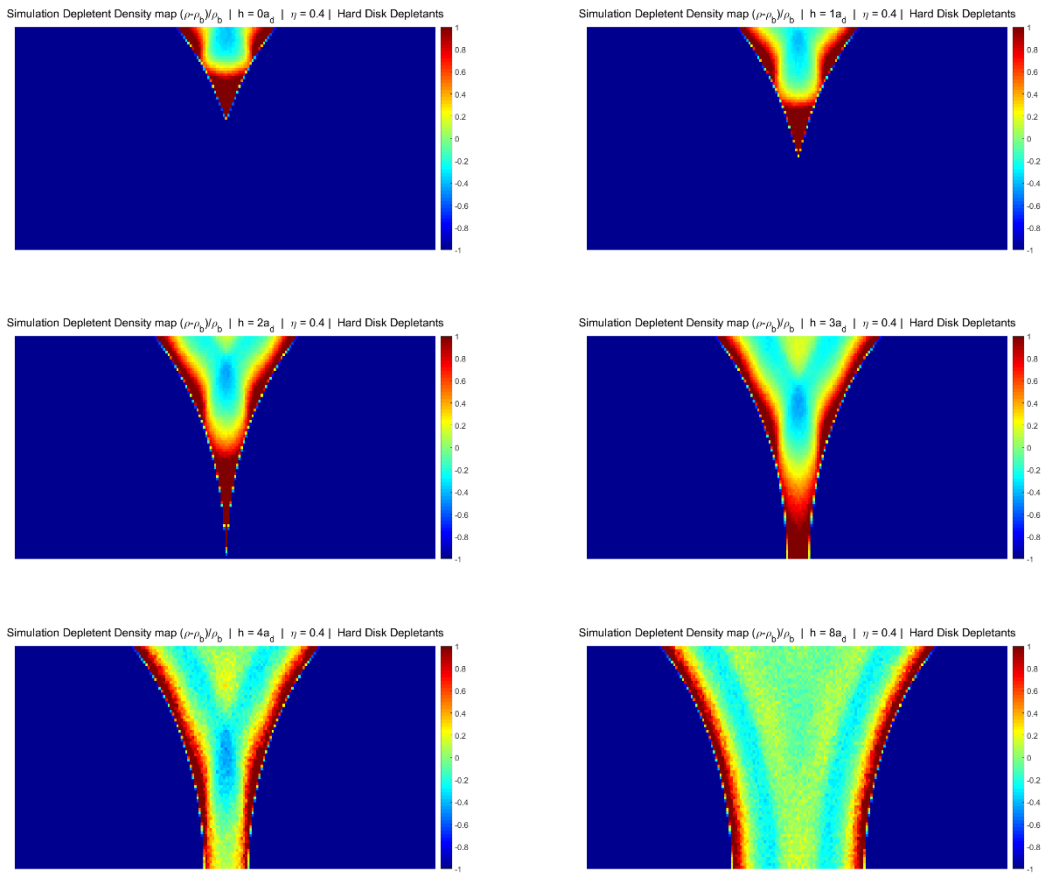

Figure 3-8: Simulation depletent density profile maps $(\rho - \rho_b)/\rho_b$. *Hard disk depletants,* $\eta = 0.4$ *Bottom right h = 8* a_d *, bottom left h = 4* a_d *, middle right h = 3* a_d *, middle left h = 2* a_d *, top right h = 1* a_d *, top left h = 0.*

Here we can see how the density profiles change as the colloids approach each other. At a separation of $8\,a_d$, the profiles have the same adsorption as $\Gamma(\infty)$. At $4a_d$ *to* $2a_d$ the density profiles of one particle start to overlap with the excluded area of the other particle. This decreases the total amount of depletents in the system. However as the colloids approach within $2\,a_d$ we see that the excluded area starts to overlap, causing adsorption.

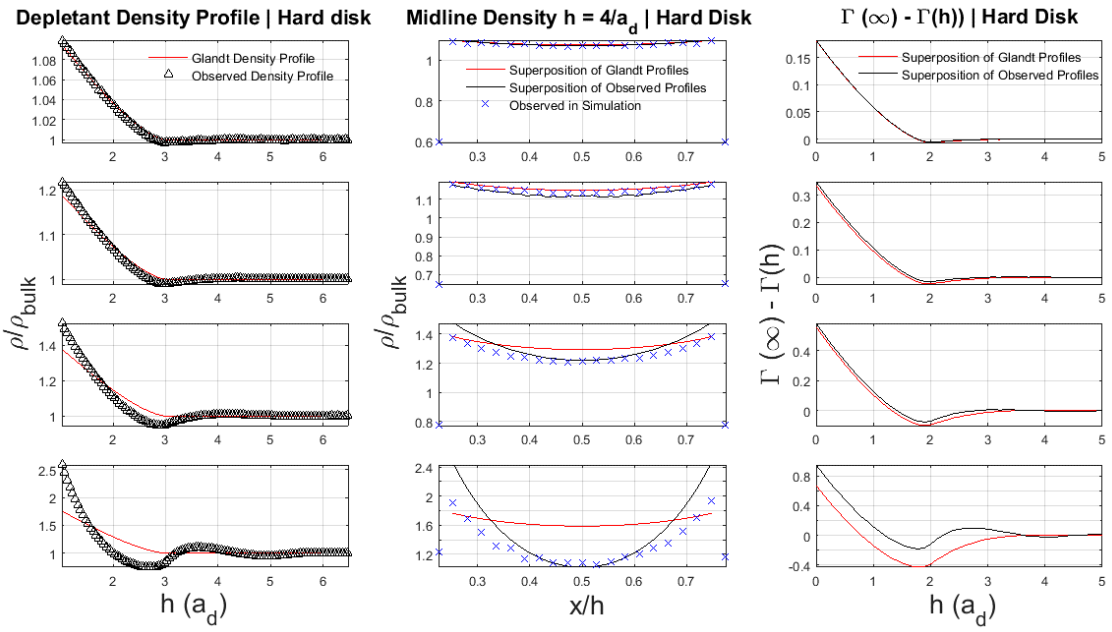

Figure 3-9: Effect of Area fraction on colloid-colloid interaction parameters with hard disk depletants. Left column: depletant density profiles ,Middle column: Depletant density at midline at h = 4 a_d , Right column: Adsorption as a function of colloid separation. Top row η *= .05, Second row* η *= 0.1, Third row* η *= 0.2, Bottom row:* η *= 0.4*

As we increase the area fraction of the system, we see the overall deviations will increase with ρ^2 , however, when viewed on a ρ / ρ_b scale, they will increase with ρ . We elected to plot the density on the midline between the colloids as we feel it will be representative of how accurate the different methods of estimating the depletent density profile are. As the area fraction increases, we see that the superposition of the density profile around one particle approach is better at estimating the true depletent density profile than the Glandt method; however there are still deviations. Turning our attention to the adsorption profile, we note desorption that occurs from $4a_d$ *to* $2a_d$. This desorption of depletents from the system causes a repulsive interaction between the colloids.

3.2.3 Colloid-colloid interaction potentials: Hard disk

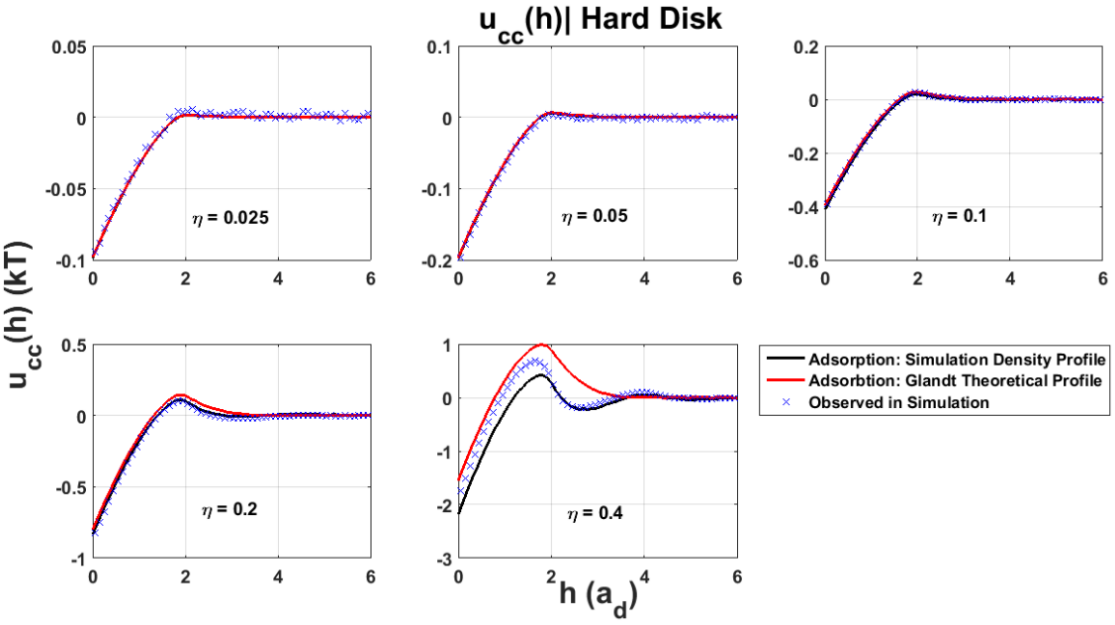

Figure 3-10: Colloid-colloid interaction potential with hard disk depletants. Red line: Adsorption theory of superimposed Glandt profiles. Black line: Adsorption theory of superimposed density profiles obtained from one particle simulations. Blue X's are obtained by simulation. Upper left η *= 0.025, Upper middle:* η *= 0.05, Upper right* η *= 0.1, Lower left:* η *= 0.2, Lower middle* η *=0.4.*

As seen in the ideal depletant case, the interaction energy increases with increasing particle density. While the non-ideal adsorption scales with ρ^2 , the interaction profiles have a depletant EOS dependent factor. The difference in contact energy between $\eta = 0.2$ and $\eta = 0.4$ is more than double. This difference is caused by the non-ideal increase in osmotic pressure of the depletants between these area fractions(25). We see above that the adsorption of the superposition of density profiles obtained from simulation was a more accurate predictor of the interaction energy than the adsorption of the superposition of Glandt density profiles, however, neither was completely accurate. We see desorption at separations of $4a_d$ *to* $2a_d$ (Figure 3-9), which translates to repulsion between the colloids. This shows a repulsive reigon between the colloids.

3.3 Attractive depletant results

Adding attractive depletant-depletant interactions allows us to more accurately capture small length scale depletion using nano-scale depletants. Unfortunately, adding attraction inhibits our ability to predict the density profiles around the colloid. As depletant-depletant attraction

increases beyond a few kT, we start to see crystallization of the depletants. Therefore we want to keep the amount of attraction low.

3.3.1 Density profile prediction: Attractive depletants

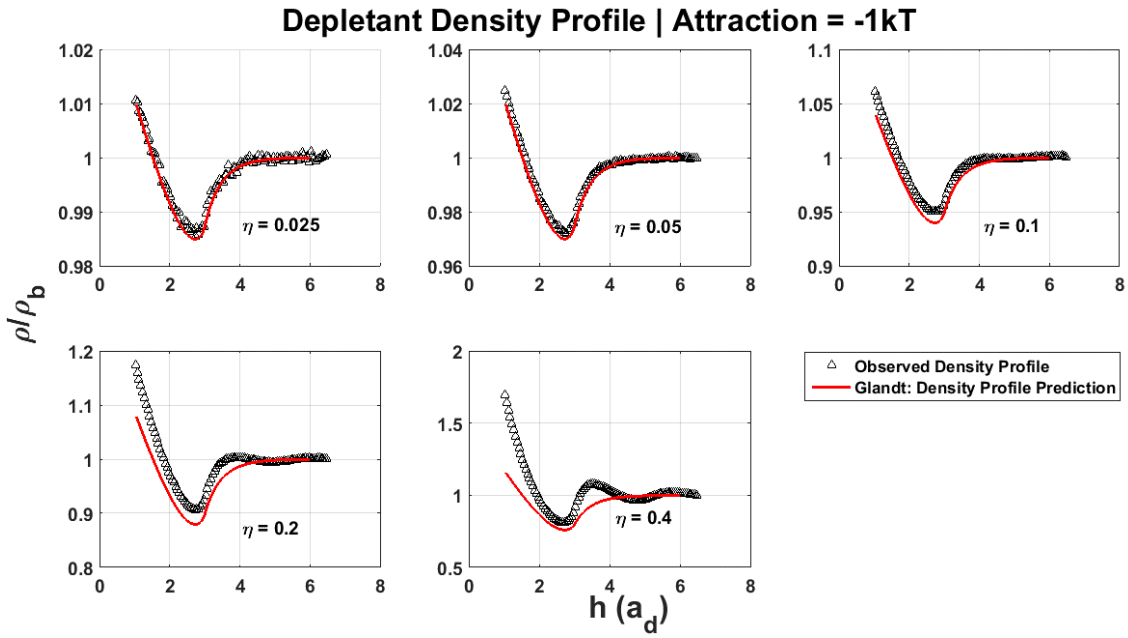

Figure 3-11: Distribution of depletants around colloid. Attraction between depletants = -1kt at contact. Red: Profile predicted by Glandt's theory. Black: Profile observed in one particle simulation. Upper left: η =0.025, Upper middle η = 0.05, Upper right η =0.1, Lower left η =0.2, Lower middle η =0.4.

As we introduce attractive depletant-depletant interactions, depletants favor being in the bulk over being close to the surface of the colloid. Intuitively, this makes sense as it would be energetically favorable for the depletants to have more near neighbors, and being near a colloid would prohibit having more neighbors. This would reduce the total amount of interaction energy available to a depletant. As was the case for the hard disk density profile, the attractive depletants with -1kt of attraction at contact have their non-idealities scale with ρ when plotted as $\rho - \rho_b$.

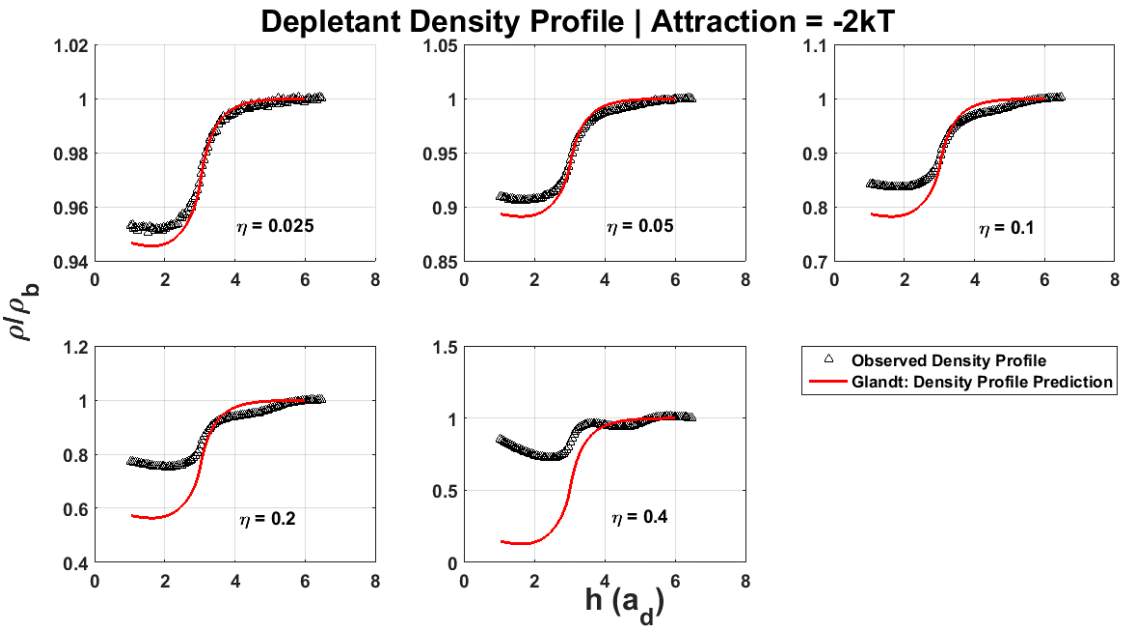

Figure 3-12: Distribution of depletants around colloid. Attraction between depletants = -2kt at contact. Red: Profile predicted by Glandt's theory. Black: Profile observed in one particle simulation. Upper left: η =0.025, Upper middle η = 0.05, Upper right η =0.1, Lower left η =0.2, Lower middle η =0.4.

When the depletant-depletant attraction is increased to -2kT at contact, we no longer see that the particles have a greater concentration near the edge of the colloid. The depletant-depletant interactions are more important to the density profile than the hard disk interactions. We see that even at η =.025, the predicted density profile is not accurate unlike the hard disk and -1kt cases. As the area fraction is increased, the deviations are even more pronounced than the previous two cases.

3.3.2 Calculating adsorption

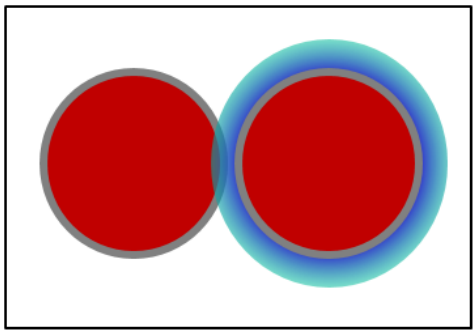

Figure 3-13: Demonstrating adsorption with attractive depletants.. The overlap of the center excluded area (red and grey) with the other colloid's excess density profile, causes a net gain of particles inside the system. The area overlapping with the excluded area has a density lower than that of bulk, causing a net migration of particles into the system.

As we start to introduce attraction between depletants, we see the depletant density profiles shift away from the colloid. The density of the depletants near the colloids is now lower than the bulk density. As these profiles start to overlap with the excluded area of the other colloid, this area is replaced at bulk density. This causes adsorption as there are now more particles in our system. This leads to long range attraction between the colloids. To visualize how these density profiles change as the colloids approach each other, we have plotted the two dimensional density profiles observed in simulation at h = 8,4,2,1,0 a_d .

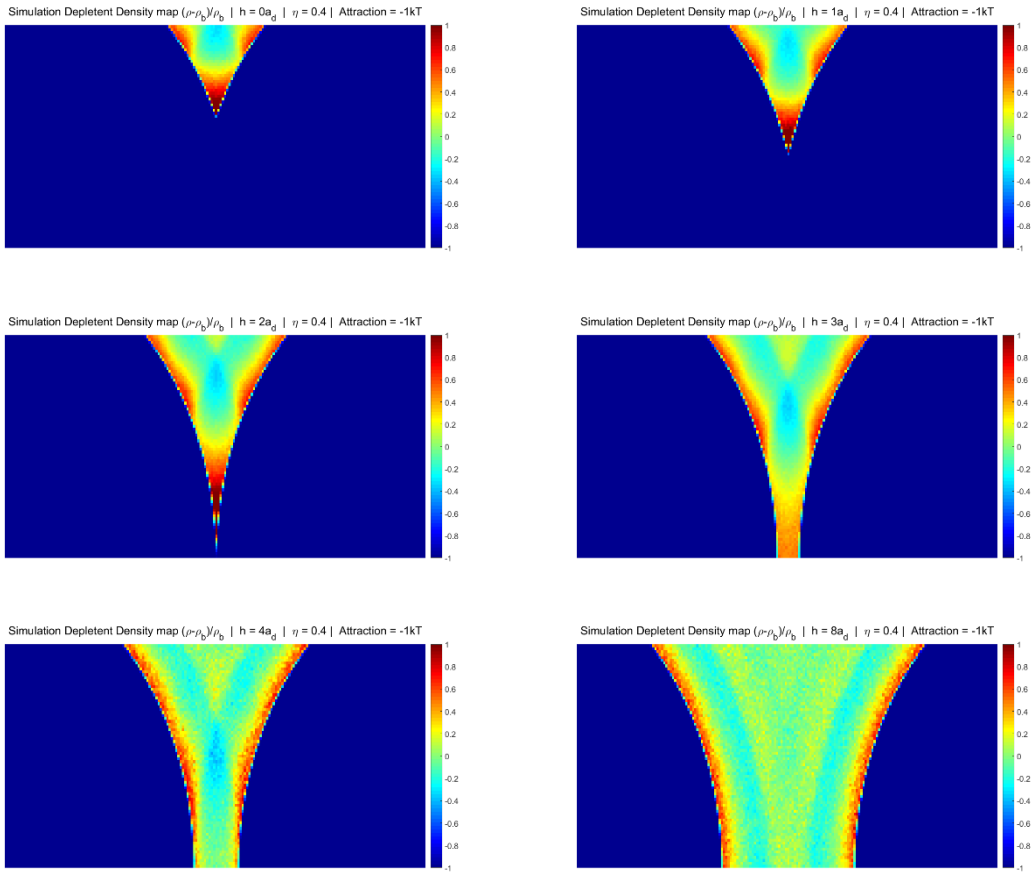

Figure 3-14: $(\rho - \rho_b)/\rho_b$ *Depletent density profile maps: Two particle simulation. -1kt attraction at contact, Bottom right h = 8* a_d *, bottom left h = 4* a_d *, middle right h = 3* a_d *, middle left h = 2* a_d *, top right h = 1* a_d *, top left h = 0* a_d *.*

Similar to the case of hard disk depletents, we see no interaction at h=8 a_d . As the colloids approach each other and the excess density profiles of one colloid overlaps with the other colloids

excluded area (dark blue), we see alternating adsorption and desorption as the density profiles are oscillatory at this high area fraction. The particle depletant density profiles are lower than the hard disc case. There is a net absorption of depletents into the system as the regions where the density is less than bulk (turquoise), overlap with the center excluded area.

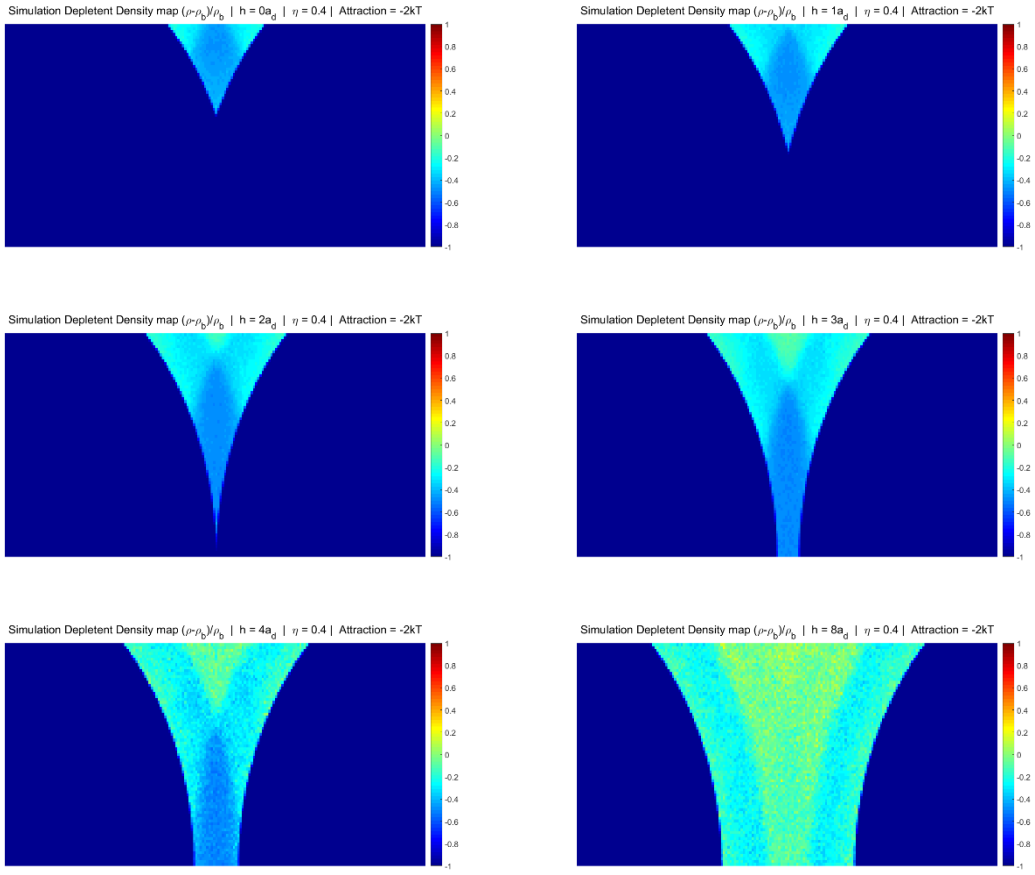

Figure 3-15: Depletent density profile maps: Two particle simulation. -2kt attraction at contact. Bottom right h = 8 a_d *, bottom left h = 4* a_d *, middle right h = 3* a_d *, middle left h = 2* a_d *, top right h = 1* a_d *, top left h = 0* a_d *.*

When attraction between depletants is increased to -2kt at contact, we see a fundamental shift in the depletant density profiles around the colloids, as depletants are no longer preferentially attracted to the surface. As the colloids move closer together, the excess density profiles are always below bulk values, which means that there is always adsorption as the excess density profiles overlap with the center excluded area. This results in long range attraction between

$5a_d$ *and* $2a_d$. Additionally, when the colloids approach within $2a_d$, the center excluded area's overlap and more particles adsorb to the system. This creates absorption of depletents at a significantly longer range than the traditional A.O. theory would predict.

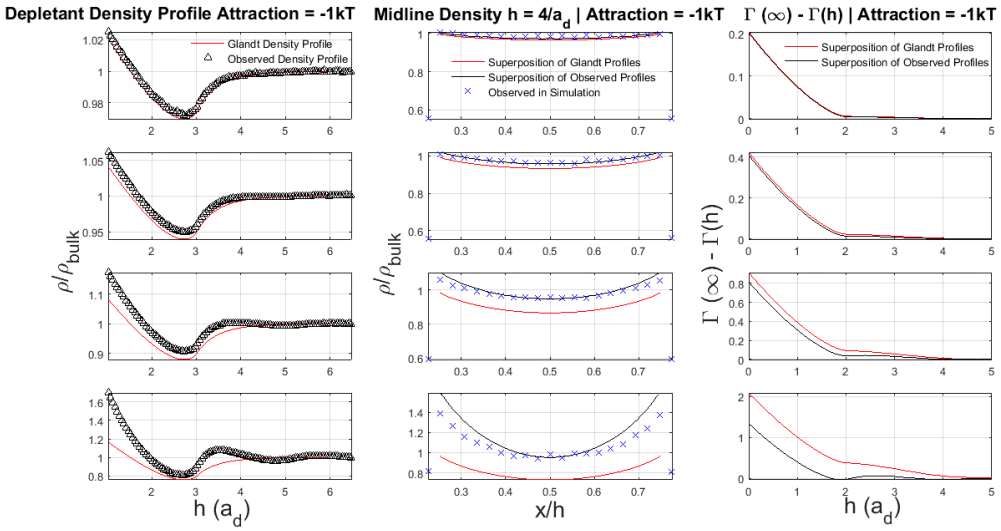

Figure 3-16: Effect of area fraction on colloid-colloid interaction parameters with -1kt of attraction between depletants. Left column: Depletant density profiles, Right column: Depletant density at midline at h = 4 a_d , Right column: Adsorption as a function of colloid separation. Top row η = .05, Second row η = 0.1, Third row η = 0.2, Bottom row: η = 0.4

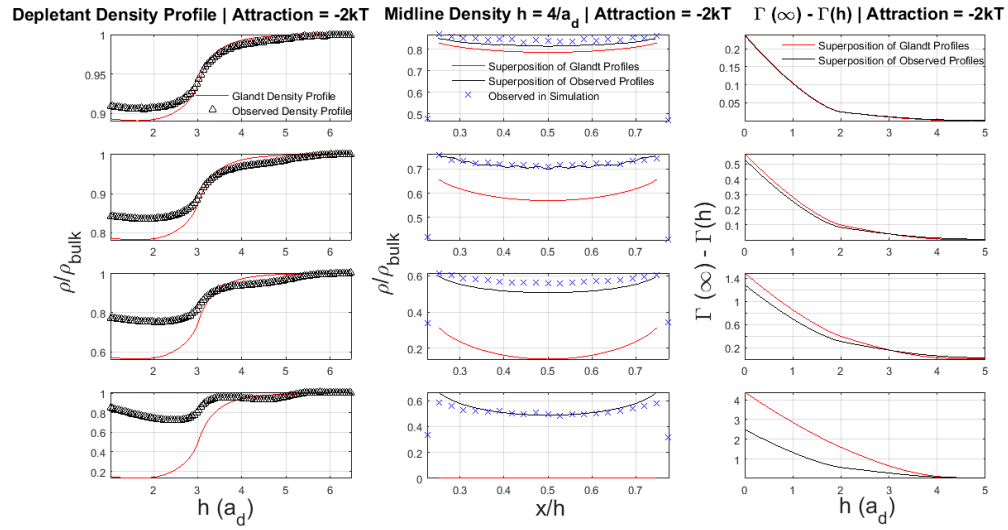

Figure 3-17: Effect of Area fraction on colloid-colloid interaction parameters with -2kt of attraction between depletants.. Left column: depletant density profiles, Right column: Depletant density at midline at h = 4 a_d , Right column: Adsorption as a function of colloid separation. Top row η = .05, Second row η = 0.1, Third row η = 0.2, Bottom row: η = 0.4

As we increase the area fraction of the system, we see that the Glandt theory does an increasingly poor job of predicting the single particle density profiles, as well as the density profiles at the midline. The Glandt profiles under-predicts the density profiles, which results in an over-prediction of adsorption. At higher area fractions, the difference in adsorption profiles between the Glandt density profiles and the superposition of density profiles is quite large, and this represents a breakdown of the theory.

Even at $\eta = 0.4$ the superposition of one particle density method is fairly accurate. We see that the adsorption is never negative, which means that the repulsive interaction seen with hard disk depletants no longer occurs. As the colloids approach each other, we see adsorption of depletants into the system, even at relatively long ranges for depletion forces. This will translate into long range attraction between colloids.

3.3.3 Colloid-colloid interaction potentials: Attractive depletants

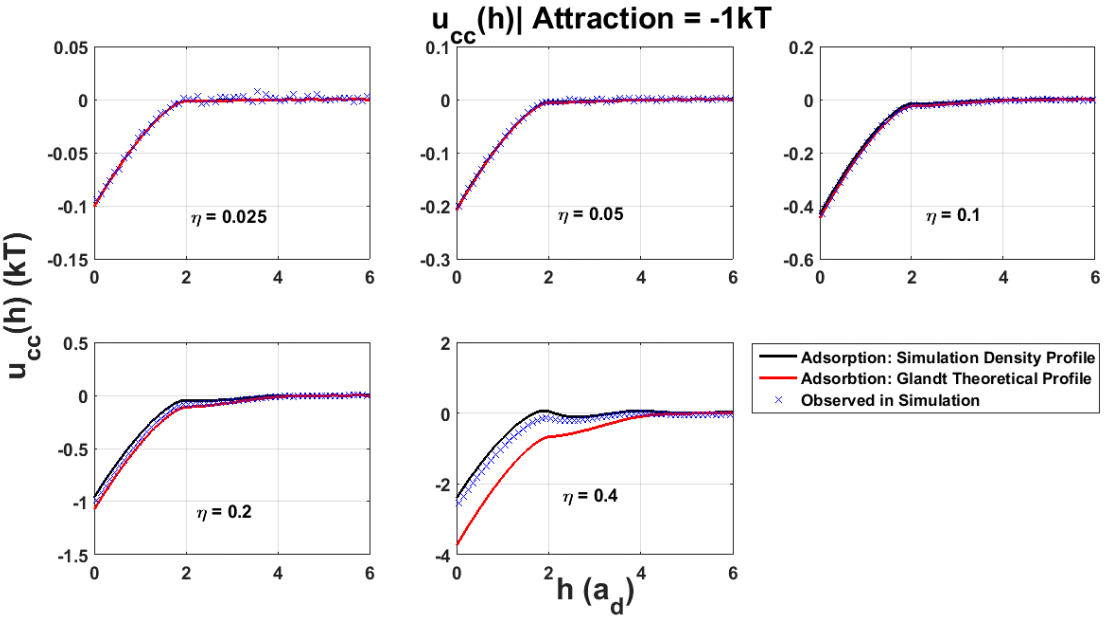

Figure 3-18: Colloid-Colloid interaction potential. Attraction between depletants = -1kt at contact. Red line: adsorption theory of superimposed Glandt profiles. Black line: adsorption theory of superimposed density profiles obtained by one particle simulations. Blue X's are obtained by simulation. Upper left η = 0.025, Upper middle: η = 0.05, Upper right η = 0.1, Lower left: η = 0.2, Lower middle η =0.4.

We see that there is adsorption between $4a_d$ and contact. As the part of the density profile that is lower than the bulk concentration overlaps with the excluded area of the other colloid, adsorption occurs and we see an attraction between the colloids. This is not very pronounced at -1kt as the density profiles are close to bulk concentration. We also notice that the oscillatory effects seen in the hard disk case have been greatly reduced. We believe this is due to a lower concentration near the surface of the colloid which leads to reduced packing effects. The attraction between depletants leads to a flatter density profile near the wall which gives a less steep and smoother adsorption profile. Again, the superposition of density profile derived from a 1 particle simulation is much more effective at accurately predicting the interaction energy.

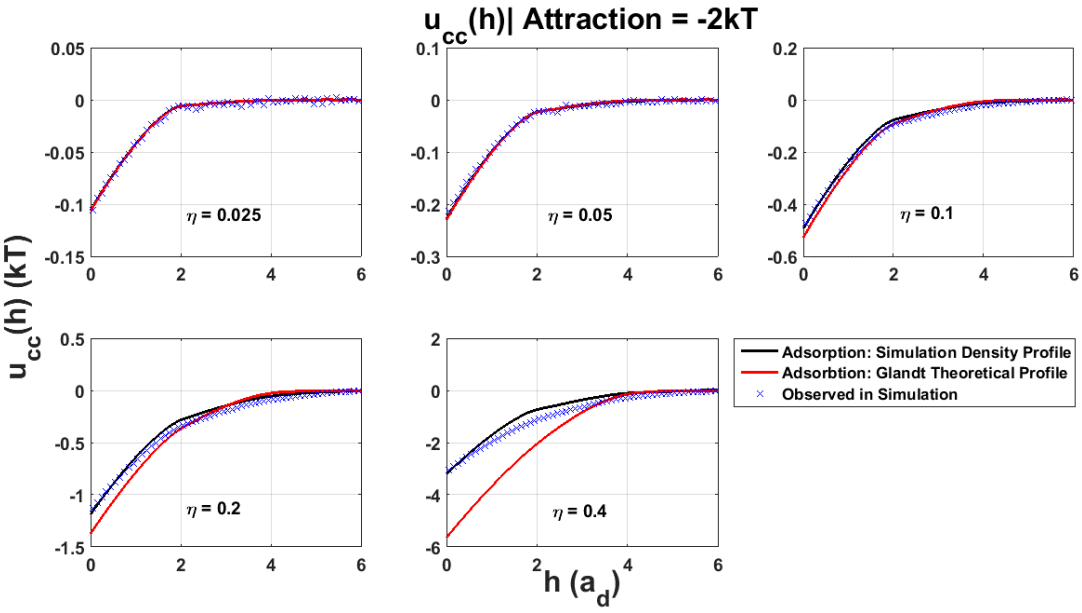

Figure 3-19: Colloid-Colloid interaction potential. Attraction between depletants = -2kt at contact. Red line: adsorption theory of superimposed Glandt profiles. Black line: adsorption theory of superimposed density profiles obtained by one particle simulations. Blue X's are obtained by simulation. Upper left η *= 0.025, Upper middle:* η *= 0.05, Upper right* η *= 0.1, Lower left:* η *= 0.2, Lower middle* η *=0.4.*

As we increase the attraction from -1kt to -2kt, the interaction energy between the colloids increases. Additionally we see a dramatic reduction in oscillatory behavior of the interaction profile at high area fraction. We believe this is due to a large reduction in the packing effects near the surface of the colloid as the particle density near the colloid is reduced. As the interaction is

longer ranged in nature, we expect this to be a good interaction to aid in single domain crystal formation.

3.4 Colloid aggregation parameters

When multiple colloids are placed at an interface, they will start to exhibit bulk behavior. As these particles may aggregate due to the attractive nature of the depletion force, we wish to investigate some of the parameters that would describe this aggregation and crystal formation, or lack thereof. Two parameters we selected were the second viral coefficient between colloids and the force between colloids at contact.

Generating a perfect 2D crystal has many applications from a negative refractive index to directionality varying band gaps, and di-electric constants[11-13]. The second virial coefficient is important to describe the thermodynamic stability of a crystal, while contact force is important to describe the ability of individual particles to change their positions within the crystal. When a crystal is forming, it is important for the colloids forming the crystal to be able to re-arrange to prevent a grain boundary from occurring. Our goal is to generate an interaction that has a very negative second virial coefficient while maintaining a low contact force as these conditions are well suited to crystal formation.

3.4.1 Force at contact between colloids

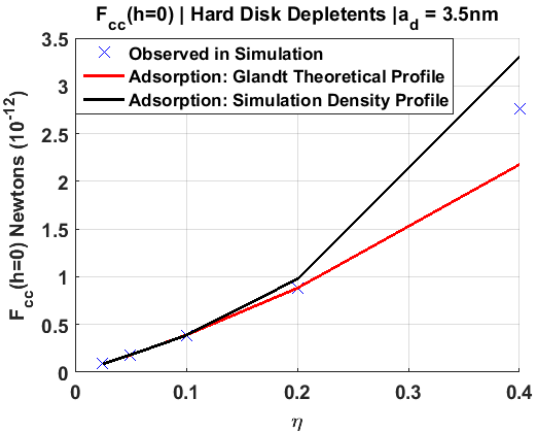

Figure 3-20: Colloid-colloid contact force for 3.5nm hard disk depletants at contact. Red: Adsorption theory prediction of the contact force using Glandt's density profiles. Black: Adsorption theory prediction of contact force using density profiles obtained from simulation. Blue X: Data points obtained from simulation.

The derivative of the interaction potential at contact is equal to the force at contact(33). If we had ideal depletants, the line of contact force versus area fraction would be linear. However, for the hard disk case we see that it curves upward. This is due to the non-linear osmotic pressure of the hard disk system. The osmotic pressure for the hard disk system increases quickly with increasing area fraction(25). This causes an increase in the interaction potential and subsequently an increase in the contact force.

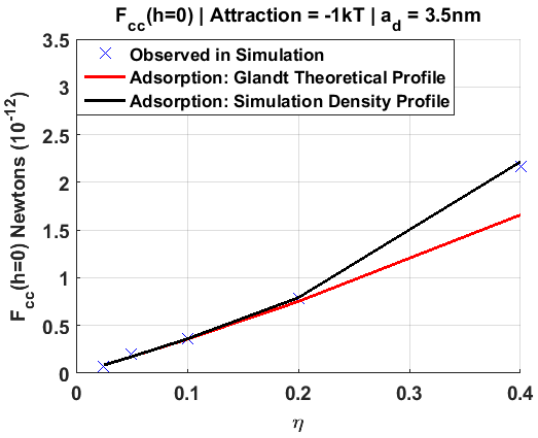

Figure 3-21: Contact Force for 3.5nm depletants with -1kt attraction at contact. Red: Adsorption theory prediction of the contact force using Glandt's density profiles. Black: Adsorption theory prediction of contact force using density profiles obtained from simulation. Blue X: Data points obtained from simulation.

Adding attraction between depletants reduces the force at contact between colloids. One reason for this reduction is the osmotic pressure of the depletants is lower for attractive systems(24). This makes the interaction potential less steep. (Figure 3-18).

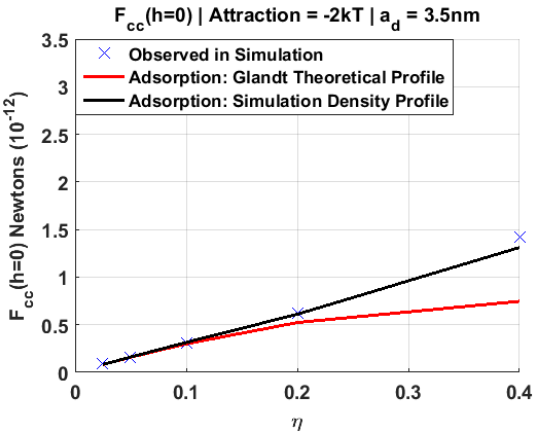

Figure 3-22: Contact Force for 3.5nm depletants with -2kt attraction at contact. Red: Adsorption theory prediction of the contact force using Glandt's density profiles. Black: Adsorption theory prediction of contact force using density profiles obtained from simulation. Blue X: Data points obtained from simulation.

For the case of -2kt attraction, the contact force is reduced further despite having a more negative contact energy. This is possible due to a combination of longer range attraction, and a reduced depletant osmotic pressure due to increased attraction between depletants.

3.4.2 Second virial coefficients of colloids

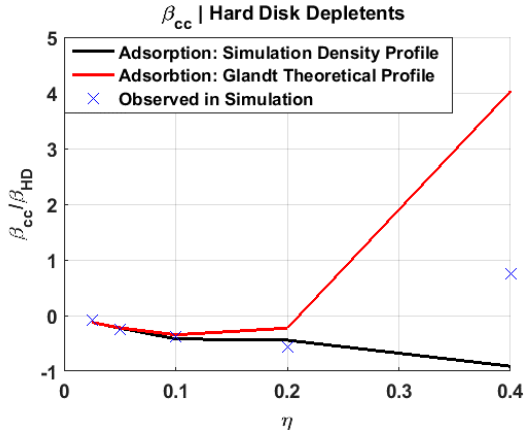

Figure 3-23:Colloid-colloid second virial coefficient with hard disk depletants .Red: Adsorption theory prediction of the second virial coefficient using Glandt's density profiles. Black: Adsorption theory prediction of the second virial coefficient using density profiles obtained from simulation. Blue X: Represents the second virial coefficient obtained from simulation.

At low concentrations, the second virial coefficient with hard disk depletants is negative. However, as the system gets more concentrated, there is a larger initial repulsion in the interaction profile. The colloids no longer favor aggregation and they are effectively stabilized at the interface. The large discrepancy between the predictions and results stems from the inability to accurately predict the interaction profile.

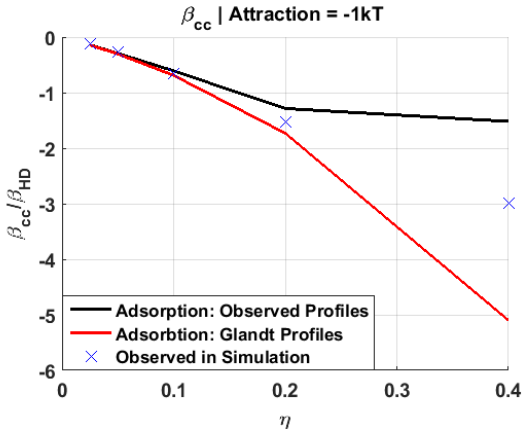

Figure : Colloid-colloid second virial coefficient with -1kt attraction between depletants. Red: Adsorption theory prediction of the second virial coefficient using Glandt's density profiles. Black: Adsorption theory prediction of the second virial coefficient using density profiles obtained from simulation. Blue X: Represents the second virial coefficient obtained from simulation.

The second virial coefficient for the case of -1kt of attraction at contact between depletants is much more negative than that of the hard disk depletants. Unlike the hard disk case, there is no repulsion in the interaction profile. This lack of positive interaction energy means that the second virial coefficient remains negative. Unfortunately our predictions of second virial coefficients at high area fractions is not very accurate.

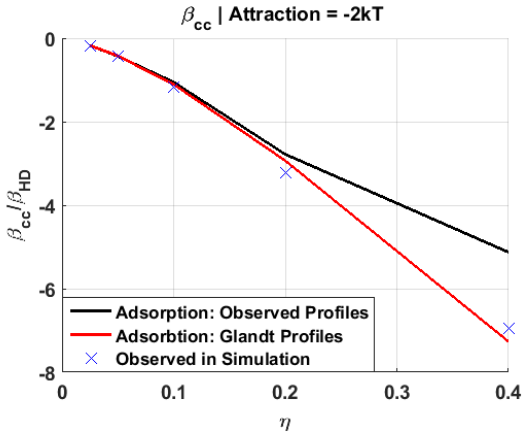

Figure 3-24: Second virial coefficients for depletants with -2kt attraction at contact. Red: Adsorption theory prediction of the second virial coefficient using Glandt's density profiles. Black: Adsorption theory prediction of the second virial coefficient using density profiles obtained from simulation. Blue X: Represents the second virial coefficient obtained from simulation.

As we increase the attraction to -2kt at contact between the depletants, the second virial coefficient becomes more negative. At high area fractions this is more pronounced. This is due to the long range attraction caused by long range adsorption. This gives a very negative second

virial coefficient and a low contact force. These are ideal traits for attempting to grow a crystal in two dimensions as they allow the individual colloids to remain bound, however they are less likely to get kinetically trapped due to the lower contact force when they are aggregated.

4 Conclusion

As we add attraction between depletants, they start to favor being in the bulk as opposed to near the surface of the colloids. Being next to a colloid limits the number of nearest neighbors a depletant can have. Because the particles want to maximize their number of nearest neighbors, they will prefer to remain in the bulk. We see this transition in (Figure 3-4,Figure 3-11, and Figure 3-12),where we progress from the hard disk case to -1kt attraction at contact between depletants, then to -2kt attraction between depletants at contact.

The hard disk depletant system has increased depletant concentration next to the colloid. This causes desorption between $4a_d$ *and* $2a_d$ as the regions of high concentration are excluded from the system. At separations less than $2a_d$ we see the excluded area regions overlap causing adsorption. This desorption at long distances creates a positive energy barrier. It is followed by a negative energy from excluded area overlap. When integrating the interaction energy profile to determine the second virial coefficient, we find that this initial energy barrier can cause the second viral coefficient to be positive, meaning that the depletion interaction in a system with hard disk depletants at high area fraction serves to stabilize the colloids.

As we add attractive depletant-depletant interactions, the concentration of depletants next to the colloid drops below bulk levels. Low densities start to be excluded and replaced by bulk density, which causes adsorption at long ranges. This adsorption gives long range attraction between colloids, and gives a flatter interaction curve. Because it is flatter, the derivative of the interaction profile at contact is lower, yielding a lower interaction energy.

When constructing 2D crystals, a negative second virial coefficient combined with a low contact force is desired. That allows the particles to correct imperfections while remaining still bound together. As the interaction profile for the -2kt system does not have a region of positive interaction energy, there is no repulsion. This lack of repulsion gives a more negative second viral coefficient, so the colloids will more readily form a crystal. Additionally, the low slope of the interaction potential lowers the derivative which results in a lower contact force. For making single domain crystals, 2D depletion at higher area fraction with attractive depletants shows promise and warrants further investigation.

5 Bibliography

1. Mao, Y.; Cates, M.; Lekkerkerker, H., Depletion Force in Colloidal Systems. *Physica A: Statistical Mechanics and its Applications* **1995**, *222*, 10-24.
2. Traube, J., Konzentrierung Von Kautschukmilchsften. *Gummi Zeitung* **1925**, *434*.
3. Bondy, C., The Creaming of Rubber Latex. *Transactions of the Faraday Society* **1939**, *35*, 1093-1108.
4. Vester, C., The Creaming of Hevea Latex by Colloids. *Rubber Chemistry and Technology* **1938**, *11*, 608-623.
5. White, H.; Frank, B. M., The Influence of Electrolyte Concentration on the Ratio of Electrosmotic to Electrophoretic Mobilities. *The Journal of Physical Chemistry* **1935**, *39*, 611-622.
6. Asakura, S.; Oosawa, F., On Interaction between Two Bodies Immersed in a Solution of Macromolecules. *Chemical Physics* **1954**, 1255-1256.
7. Asakura, S.; Oosawa, F., Interaction between Particles Suspended in Solutions of Macromolecules. *Journal of polymer science* **1958**, *33*, 183-192.
8. Glandt, E. D., Density Distribution of Hard—Spherical Molecules inside Small Pores of Various Shapes. *Journal of Colloid and Interface Science* **1980**, *77*, 512-524.
9. Walz, J. Y.; Sharma, A., Effect of Long Range Interactions on the Depletion Force between Colloidal Particles. *Journal of colloid and interface science* **1994**, *168*, 485-496.
10. Israelachvili, J. N., *Intermolecular and Surface Forces: Revised Third Edition*; Academic press, 2011.
11. Engheta, N.; Ziolkowski, R. W., *Metamaterials: Physics and Engineering Explorations*; John Wiley & Sons, 2006.
12. Joannopoulos, J. D.; Johnson, S. G.; Winn, J. N.; Meade, R. D., *Photonic Crystals: Molding the Flow of Light*; Princeton university press, 2011.
13. Whitesides, G. M.; Grzybowski, B., Self-Assembly at All Scales. *Science* **2002**, *295*, 2418-2421.
14. Biben, T.; Ohnesorge, R.; Löwen, H., Crystallization in Sedimentation Profiles of Hard Spheres. *EPL (Europhysics Letters)* **1994**, *28*, 665.
15. van Blaaderen, A.; Wiltzius, P., Growing Large, Well-Oriented Colloidal Crystals. *Advanced Materials* **1997**, *9*, 833-835.
16. Yethiraj, A.; Thijssen, J. H.; Wouterse, A.; van Blaaderen, A., Large-Area Electric-Field-Induced Colloidal Single Crystals for Photonic Applications. *Advanced materials* **2004**, *16*, 596-600.
17. Edwards, T. D.; Beltran-Villegas, D. J.; Bevan, M. A., Size Dependent Thermodynamics and Kinetics in Electric Field Mediated Colloidal Crystal Assembly. *Soft Matter* **2013**, *9*, 9208-9218.
18. Lin, K.-h.; Crocker, J. C.; Prasad, V.; Schofield, A.; Weitz, D. A.; Lubensky, T.; Yodh, A., Entropically Driven Colloidal Crystallization on Patterned Surfaces. *Physical review letters* **2000**, *85*, 1770.
19. Tuinier, R.; Vliegenthart, G. A.; Lekkerkerker, H. N., Depletion Interaction between Spheres Immersed in a Solution of Ideal Polymer Chains. *The Journal of Chemical Physics* **2000**, *113*, 10768-10775.
20. Backus, J. In *The History of Fortran I, Ii, and Iii*, History of programming languages I, ACM: 1978; pp 25-74.
21. Hansen, J.-P.; McDonald, I. R., *Theory of Simple Liquids*; Academic Press, 1976. pg.58
22. Manousiouthakis, V. I.; Deem, M. W., Strict Detailed Balance Is Unnecessary in Monte Carlo Simulation. *The Journal of chemical physics* **1999**, *110*, 2753-2756.

23. Wood, W. W.; Jacobson, J., Preliminary Results from a Recalculation of the Monte Carlo Equation of State of Hard Spheres. *The Journal of Chemical Physics* **1957**, *27*, 1207-1208.
24. Laurendeau, N. M., *Statistical Thermodynamics: Fundamentals and Applications*; Cambridge University Press, 2005.
25. Mravlak, M., Depletion Force. *University of Ljubljana* **2008**, 3-6.
26. Alder, B.; Wainwright, T., Phase Transition for a Hard Sphere System. *The Journal of chemical physics* **1957**, *27*, 1208.
27. Parsegian, V. A.; Weiss, G. H., Spectroscopic Parameters for Computation of Van Der Waals Forces. *Journal of Colloid and Interface Science* **1981**, *81*, 285-289.
28. Sphere-Sphere Intersection. http://mathworld.wolfram.com/Sphere-SphereIntersection.html (accessed 7/24/15).
29. Circle-Circle Intersection. http://mathworld.wolfram.com/Circle-CircleIntersection.html (accessed 7/24/15).
30. Beltran-Villegas, D. J.; Sehgal, R. M.; Maroudas, D.; Ford, D. M.; Bevan, M. A., Colloidal Cluster Crystallization Dynamics. *The Journal of chemical physics* **2012**, *137*, 134901.
31. Baker, J.; Henderson, D., Perturbation Theory and Equation of State for Fluids: The Square-Well Potential. *J Chem Phys* **1967**, *47*, 2856-2861.

6 Appendix 1: Force balance around colloids

$$\cos(\theta_1) = \frac{h + 2a_c}{2R}$$

$$\theta_1 = \cos^{-1}\frac{h + 2a_c}{2R}$$

$$\theta_1 = \cos^{-1}\left(\frac{h + 2a_p}{2\left(a_p + a_d\right)}\right)$$

To find the average force in the x direction, we need to find the average of the x component over the arc.

$$2\Pi \int_{\pi}^{\pi-\theta_1} \cos(\theta) d\theta = \frac{\Pi \sin(\theta_1)}{\theta_1} \quad (36)$$

$$F_{cc}\left(h\right) = \frac{\Pi \sin(\theta_1)}{\theta_1} * 2 * \frac{\theta_1}{2\pi} * 2\pi\left(a_c + a_d\right) = 2\left(a_c + a_d\right)\Pi \sin\left(\cos^{-1}\left(\frac{h + 2a_c}{2\left(a_c + a_d\right)}\right)\right)$$

$$\int_{2(_d}^{h_1} F_{cc}(\mathrm{h})\,\mathrm{dh} = u_{cc}(\mathrm{h}_1)$$

$$u_{cc}(\mathrm{h}) = \int_{2a_d}^{h_1} 2\left(a_c + a_d\right)\Pi \sin\left(\cos^{-1}\left(\frac{h + 2a_c}{2\left(a_c + a_d\right)}\right)\right) = \frac{\left(a_c + a_d\right)\Pi}{2}\left(d\sqrt{4 - \frac{\left(h + 2a_c\right)^2}{\left(a_c + a_d\right)^2}} + 4\left(a_c + a_d\right)\sin^{-1}\left(\frac{h + 2a_c}{2\left(a_c + a_d\right)}\right)\right)\Big|_{2a_d}^{h_1}$$

$$u_{cc}(\mathrm{h}_1) = \frac{\left(a_c + a_d\right)\Pi}{2}\sqrt{4\left(a_c + a_d\right)^2 - \left(h_1 + 2a_c\right)^2} + \Pi 2\left(a_c + a_d\right)^2 \cos^{-1}\left(\frac{\left(h_1 + 2a_c\right)}{2\left(a_c + a_d\right)}\right) = -\Pi\Delta A$$

$$u_{cc}(\mathrm{h}) = \int_{2R}^{d_1} 2\left(a_c + a_d\right)\Pi \sin\left(\cos^{-1}\left(\frac{h + 2a_c}{2\left(a_c + a_d\right)}\right)\right)$$

$$U_{cc}(\mathrm{h}) = \frac{\left(a_c + a_d\right)\Pi}{2}\left(\left(h + 2a_c\right)\sqrt{4 - \frac{\left(h + 2a_c\right)^2}{\left(a_c + a_d\right)^2}} + 4\left(a_c + a_d\right)\sin^{-1}\left(\frac{\left(h + 2a_c\right)}{2\left(a_c + a_d\right)}\right)\right)\Big|_{2\left(a_c + a_d\right)}^{h_1}$$

$$u_{cc}(\mathrm{h}) = \Pi\left(2\left(a_d + a_c\right)^2 \cos^{-1}\left(\frac{h + 2a_c}{2\left(a_c + a_d\right)}\right) - \frac{\left(h + 2a_c\right)}{2}\sqrt{4\left(a_c + a_d\right)^2 - \left(h + 2a_c\right)^2}\right)$$

7 Appendix 2: Reducing number of dimensions of the A.O. theory

When calculating the interaction potential of two different size disks for depletion forces, the absolute sizes of the particles are unimportant, but rather the size ratio of the particles are important.

The A.O. theory equations:

$$u_{cc}(\mathrm{h}) = \Pi * \Delta A$$

$$\Pi = \rho kT$$

$$\rho * \pi * a_d^2 = \eta$$

$$\rho = \pi a_d^2 \eta$$

$$\Delta A = \left(2\left(a_d + a_c\right)^2 \cos^{-1}\left(\frac{h + 2a_p}{2\left(a_c + a_d\right)} \right) - \frac{\left(h + 2a_c\right)}{2} \sqrt{4\left(a_c + a_d\right)^2 - \left(h + 2a_c\right)^2} \right)$$

Putting the previous equations together

$$U_{cc}(h) = \frac{\eta kT}{\pi a_d^2} \left(2\left(a_d + a_p\right)^2 \cos^{-1}\left(\frac{h + 2a_p}{2\left(a_c + a_d\right)} \right) - \frac{\left(h + 2a_c\right)}{2} \sqrt{4\left(a_c + a_d\right)^2 - \left(h + 2a_c\right)^2} \right)$$

Now, we define the separations in terms of the radii of the depletants, and a dimensionless size ratio.

$$let:\ h' = \frac{h}{a_d}\ ,\ a_c' = \frac{a_c}{a_d}$$

$$U_{cc}(\mathrm{h}) = \frac{\eta kT}{\pi a_d^2} \left(2a_d^2 \left(a_c' + 1\right) \cos^{-1}\left(\frac{h a_d + 2a_c' a_d}{2\left(a_c' a_d + a_d\right)} \right) - \frac{\left(h' a_d + 2a_c' a_d\right)}{2} \sqrt{4a_d^2 \left(a_c' + 1\right)^2 - a_d^2 \left(h + 1\right)^2} \right)$$

$$U_{cc}(\mathrm{h}) = \frac{\eta kT}{\pi} \left(2\left(a_c' + 1\right) \cos^{-1}\left(\frac{h' + 2a_c'}{2\left(a_c' + 1\right)} \right) - \frac{\left(h' + 2a_c'\right)}{2} \sqrt{4\left(a_c' + 1\right)^2 - \left(h' + 1\right)^2} \right)$$

Here we see that interaction energy of the colloids is not dependent on their absolute sizes, but rather their relative sizes.

8 Appendix 3: Derivation of 2D second virial coefficient

$$\beta_{3D} = -2\pi \int_0^{\infty} \left(\exp\left(\frac{u(\mathrm{r})}{kT} \right) - 1 \right) r^2 dr$$

Converting the laplacian:

$$\frac{4}{3}\pi(\mathrm{r}+\Delta \mathrm{r})^3 - \frac{4}{3}\pi r^3$$

$$\frac{4}{3}\pi(\mathrm{r}^3 + 3r^2\Delta r + 3r\Delta r^2 + \Delta \mathrm{r}^3) - \frac{4}{3}\pi r^3$$

Cancel any terms that are as small as Δr^2 can be neglected

$$\frac{4\pi}{3}\left(r^3 + 3r^3\Delta r\right) - \frac{4\pi}{3} r^3 = 4\pi r^2 \Delta r$$

The shell of a disk is:

$$\pi\left(r + \Delta r\right)^2 - \pi r^2 = 2\pi r \Delta r$$

From this, we can determine that the second virial coefficient in 2D is:

$$\beta_{2D} = -\pi \int_0^{\infty} \left(\exp\left(\frac{u(\mathrm{r})}{kT} \right) - 1 \right) r \; dr$$

9 Curriculum Vitae

Maxwell Pinz

Permanent Address: N7371 jungle lane Waterloo WI, 53594

Email / phone: Mpinz109@gmail.com / 920-344-9352

Education

Master of Science in Chemical and Biomolecular Engineering	September 2015
Bachelor of Science in Applied Mathematics and Statistics (Concentration: Optimization)	May 2014
Bachelor of Science in Chemical and Biomolecular Engineering (Concentration: Interfaces and Nanotechnology)	May 2014